Chapter 64

Haploinsufficiency of *STXBP1* and Ohtahara Syndrome

Hirotomo Saitsu
Mitsuhiro Kato
Naomichi Matsumoto

INTRODUCTION

Ohtahara syndrome (OS), also known as *early infantile epileptic encephalopathy with suppression-burst*, is one of the most severe and earliest forms of epilepsy.[1] It is characterized by early onset of tonic seizures, seizure intractability, characteristic suppression-burst patterns on the electroencephalogram (EEG), and a poor outcome with severe psychomotor retardation.[2,3] Brain malformations, such as cerebral dysgenesis or hemimegalencephaly, are often associated with OS, but cryptogenic or idiopathic OS is found in a subset of OS patients, in whom genetic aberrations might be involved.[4] Although mutations of the *ARX* gene have been found in several male patients with OS,[5–8] the genetic causes are unexplained in most cryptogenic OS cases. We have recently found de novo mutations in *STXBP1* (encoding syntaxin binding protein 1, also known as MUNC18-1) in individuals with cryptogenic OS.[9] Here we present all the mutations in *STXBP1* found to date in OS patients, as well as some evidence of mutations leading to haploinsufficiency.

OHTAHARA SYNDROME

Ohtahara syndrome was first reported as the earliest form of age-dependent epileptic syndromes by Ohtahara et al.[1] It is characterized by early onset of intractable tonic spasms, characteristic suppression-burst patterns on interictal EEG, and a poor outcome with severe psychomotor retardation.[2,3] According to a previous report,[4] all patients have seizure onset within the first 3 months, with the majority (75%) in the first month. Tonic spasms were observed in all patients. One-third to one-half of patients also had partial seizures, such as erratic focal motor seizures and hemiconvulsions, or asymmetric tonic seizures; however, myoclonic seizures were rare. Hemiconvulsions, tonic seizures, or clonic seizures precede the onset of tonic spasms by 1 to several weeks to in 37.5% of OS patients.[4] Brain malformations, such as cerebral dysgenesis, hemimegalencephaly, porencephaly, and Aicardi syndrome, are often associated with OS, but a significant proportion of patients (31% to 50% of OS cases) remain etiologically unexplained.[2,4] Suppression-burst patterns on interictal EEG consisting of high-voltage activity alternating with nearly flat suppression phases are observed when the patient is both awake and asleep.

Early myoclonic encephalopathy (EME) is another epileptic syndrome showing suppression-burst patterns on EEG.[10] The prevailing initial seizure type is a main difference between OS and EME: tonic seizures in OS and myoclonic seizures in EME.[2,3] However, OS and EME have common features, and it is often difficult to distinguish between them. Homozygous missense mutations of the *SLC25A22* (mitochondrial glutamate carrier 1) gene have been recently found in EME individuals in consanguineous families.[11,12] Age-dependent evolution is a characteristic feature of both OS and EME: approximately 75% and 40% of OS and EME cases, respectively, transit to West syndrome (WS), usually 3–4 months afterward.[2,3] West syndrome is characterized by tonic spasms with clustering, arrest of psychomotor development, and hypsarrhythmia on EEG. Such transitions suggest a common pathophysiology between OS and WS or between EME and WS. Consistent with this hypothesis, specific mutations of the *ARX* (*aristaless*-related homeobox) gene at Xp22.13, have been recently found in male OS and WS cases.[5–8,13–15]

DE NOVO *STXBP1* MUTATIONS CAUSE OS

Identification of *STXBP1* Mutations in Patients with OS

Through BAC array-based comparative genomic hybridization analysis of patients associated with mental retardation (MR), we found a microdeletion at 9q33.3-q34.11 in a female patient with OS.[9] As the microdeletion occurred de novo, we assumed that a gene within the deletion was responsible for OS. Among the genes mapped within the deletion, the gene encoding syntaxin binding protein 1 (STXBP1) was of particular interest because mouse *Stxbp1* has been shown to be essential for synaptic vesicle release[16] and is specifically expressed in the brains of rodents and humans.[17,18] We therefore analyzed *STXBP1* in 13 unrelated patients with OS. Four heterozygous missense mutations were found at evolutionarily conserved amino acids in three males and one female (Fig. 64–1 and Table 64–1). Three mutations were confirmed as de novo events (paternal DNA was unavailable for one remaining mutation).

STXBP1 Mutation Is a Major Genetic Cause of OS

To delineate the clinical spectrum of patients with *STXBP1* mutations, *STXBP1* was further analyzed in 29 and 54 cases of cryptogenic OS and WS, respectively.[19] No brain malformations were found in any of the cases. Seven novel heterozygous mutations were found in nine OS cases (the same mutation was found in three cases), but none in WS cases (six males and three females; Fig. 64–1 and Table 64–1). The mutations included one missense, one splicing, two frameshift, and three nonsense mutations. A recurrent missense mutation (c.1217G>A, p.R406H) occurred at an evolutionarily conserved amino acid (Fig. 64–1). All the mutations occurred de novo. Collectively, *STXBP1* aberrations account for about one-third of individuals with OS (14 out of 43). These data showed that *STXBP1* mutations are a major genetic cause of cryptogenic OS, but they are not a genetic cause of WS in our Japanese cohort.

Clinical Features of Patients with *STXBP1* Deletion/Mutations

Clinical information from 14 individuals with confirmed *STXBP1* deletion/mutations is summarized in Table 64–1. These persons showed

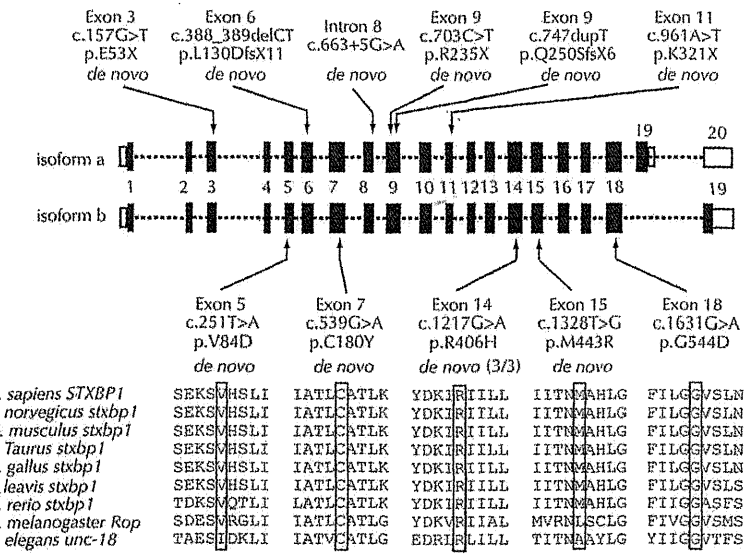

Figure 64–1. Summary of *STXBP1* mutations found in Japanese individuals with OS. Schematic representation of STXBP1, consisting of at most 20 exons (the UTR and the coding region are open and filled rectangles, respectively). There are two isoforms, a (GenBank accession number, NM_003165) with exon 19, and b (NM_001032221) without exon 19 of isoform a. Locations of mutations are indicated by arrows. Eleven different mutations are presented: missense mutations are indicated below the gene scheme, and the other types of mutations are indicated above the gene. Ten mutations in 12 subjects occurred de novo. All missense mutations occurred at evolutionarily conserved amino acids. CLUSTALW (http://align.genome.jp/) was used to align homologs of different species. Adapted from refs. 9 and 19.

distinctive features of OS, such as early-onset seizures including epileptic spasms, suppression-burst pattern on EEG, transition to WS after a few to several months, and severe developmental delay. Epileptic spasms were preceded by other seizure types, including partial seizures in 11 subjects. Transition to WS was observed in 11 subjects with OS. Although seizures were intractable in nine subjects, five subjects responded to medication, such as thyrotropin-releasing hormone (TRH) injection, adrenocorticotropic hormone (ACTH) injection, vitamin B_6, high-dose phenobarbital, and valproic acid. All subjects demonstrated severe psychomotor developmental delay. Brain magnetic resonance imaging (MRI) showed no structural anomalies or hippocampal anomalies but did show some atrophy (Fig. 64–2A). Suppression-burst on interictal EEG was observed in both awake and asleep states (Fig. 64–2B). We gained several insights into the phenotype of *STXBP1* aberrations. Firstly, the age at onset of epileptic spasms is later in subjects with *STXBP1* aberrations than in the 16 original subjects reported by Yamatogi and Ohtahara.[4] Only 27% of the subjects (4/15) in our series had onset of OS within 1 month compared to 75% (12/16) in the series of Yamatogi and Ohtahara. As subjects with *STXBP1* aberrations showed no structural anomalies on brain MRI examination, the onset of epileptic seizures might be affected by associated structural brain abnormalities, which are commonly seen in other reports of OS. Secondly, myoclonic seizures, which are thought to be rarely observed in OS, were occasionally observed (3/14). Myoclonic seizures are the main ictal symptom of EME. These three subjects can be diagnosed as having EME when myoclonic seizures dominate. Thus, *STXBP1* might also be causative for EME, implying a genetic linkage between OS and EME. Another infrequent but interesting finding is that one patient (no. 5) developed vigorous chorea-ballismus

Table 64–1 Summary of Clinical Features of Subjects with STXBP1 Deletion/Mutations

Case # Mutation	Initial Symptoms	Onset of Spasms	Transition from Spasms to Other Seizures	Response to Therapy
#1 Deletion	Tonic seizure and oral automatism	2 m	Generalized clonic seizure at 29 m	Seizure free from 5 m after TRH injection
#2 c.1631G>A	Blinking	10 d	No	Seizure free from 3 m
#3 c.539G>A	Tonic seizure with blinking	3 m	No	Intractable, daily
#4 c.1328T>G	Upward gazing and tonic seizure	2 m	Partial seizure at 8 m	Intractable, hourly TRH injection was temporally effective
#5 c.251T>A	Spasms and tonic-clonic seizure	2 m	No	Intractable, daily
#6 c.1217G>A	Generalized convulsions	3 w	No	Intractable, hourly
#7 c.1217G>A	GTCS with upward eye gazing	2 m	Myoclonic seizure at 48 d	Intractable, daily
#8 c.1217G>A	Partial seizures (right hemiconvulsion)	2 m	Tonic seizure to myoclonic seizure	Intractable, daily
#9 c.157G>T	Spasms	2 d	Versive seizure after hypoxia at 2 y	Intractable, daily
#10 c.388_389del	Secondary generalized seizures	2 m	CPS	Seizure free after ACTH or VPA with KBr
#11 c.663+5G>A	Blinking to tonic seizures	1 m	Tonic seizure	Seizure free with VB6 for spasms and ACTH for WS
#12 c.703C>T	Spasms in cluster	1 m	No	Seizure free from 6 m after high-dose PB
#13 c.747dup	Clonic convulsion	31 d	Partial seizure and myoclonic seizures	Intractable, hourly
#14 c.961A>T	Partial seizures	3 w	Partial seizure	Intractable, daily

GTCS, generalized tonic-clonic seizures; CPS, complex partial seizure; TRH, thyrotropin-releasing hormone; ACTH, adrenocorticotropic hormone; VPA, valproic acid; KBr, potassium bromide; VB6, vitamin B_6; PB, phenobarbital; d, day(s); w, week; m, month(s); y, year(s); 0 w, 0 to 6 days; 0 m, 0 to 3 weeks.

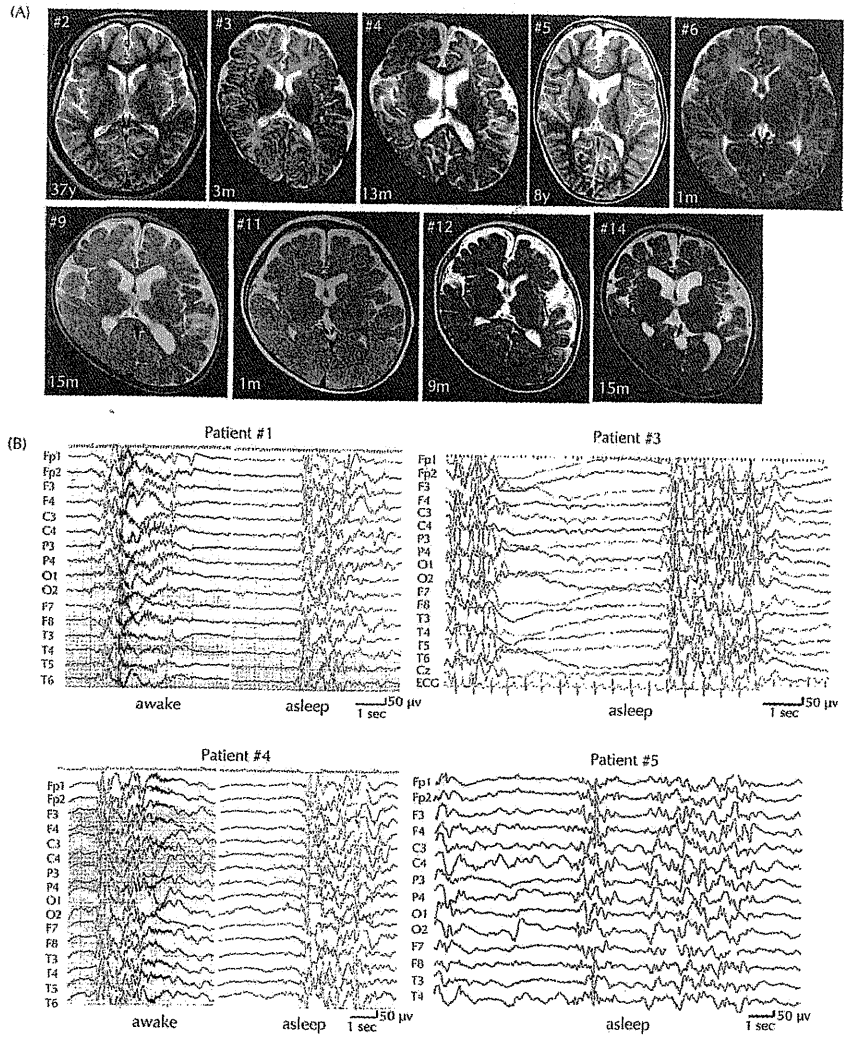

Figure 64–2. Brain MRI scan and EEG of OS patients with *STXBP1* aberrations. **A.** Brain MRI (T2-weighted axial) image through the basal ganglia shows normal brain structure in patients with *STXBP1* mutations. Patient IDs and developmental stages are indicated. Mild dilatation of lateral ventricles is observed in patients #4, #9, #11, and #14, but none shows brain malformation. y, year(s); m, month(s). **B.** Suppression-burst on interictal EEG of patients 1 (at age 2 months), 3 (at 3 months), 4 (at 2 months), and 5 (at 3 months). High-voltage bursts alternating with almost flat suppression phases at an approximately regular rate in both awake and asleep states. Adapted from refs. 9 and 19.

subsequent to OS, suggesting that mutations of *STXBP1* could affect the basal ganglia.[9,20] In terms of the genotype–phenotype relationship, we found no difference in clinical data between seven subjects with missense mutations and seven subjects with microdeletions, premature termination codons, or splicing mutations. This finding is supported by our experimental data that demonstrated both missense mutations and a splicing mutation resulted in haploinsufficiency of *STXBP1*: degradation of STXBP1 proteins containing missense mutations and nonsense-mediated mRNA decay (NMD) associated with aberrantly spliced mRNAs (see below).

MOLECULAR EVIDENCE OF *STXBP1* HAPLOINSUFFICIENCY

Mutant STXBP1 Proteins Are Unstable

All five missense mutations lead to amino acid replacements in the hydrophobic core of STXBP1 and are considered to destabilize the folding architecture. This is especially true for the three mutants (p.V84D, p.G544D, and p.M443R) that have replaced the wild-type (WT) residues with charged residues, which would be predicted to severely disrupt the conformation of STXBP1.[9] In fact, circular dichroism (CD) spectra showed that the helical content of the C180Y mutant is lower (39%) than that of the WT (43%), suggesting that the mutation destabilized the secondary structure of STXBP1[9] (Fig. 64–3A). Moreover, CD melting experiments revealed that the melting temperature (T_m) of the C180Y mutant was about 11 degrees lower than that of the WT (Fig. 64–3B), indicating that the C180Y mutant is much more unstable than the WT. The regulation of synaptic vesicle release by Stxbp1 is mediated in part by binding to Syntaxin-1A as well as directly to the soluble *N*-ethylmaleimide-sensitive factor attachment protein receptor (SNARE) complex, which mediates fusion of vesicles with the target membrane.[21,22] Binding of a mutant protein (p.C180Y) to syntaxin-1A was also significantly impaired, even at 4°C in vitro.[9] Together with the fact that the T_m of the C180Y mutant is close to the physiological temperature of the human body, it is less likely that its functional activity could be retained in the human brain. Other STXBP1 mutants (p.V84D, p.G544D, and p.M443R) tend to form aggregates, and thus sufficient protein for biophysical analyses could not be obtained.

Degradation of Mutant *STXBP1* Proteins

Transient expression of mutant STXBP1 proteins in Neuroblastoma 2A (N2A) cells showed further evidence of *STXBP1* haploinsufficiency. The WT EGFP-STXBP1 was expressed in the cytosolic compartment, but not in the nucleus or plasma membrane, similar to endogenous expression.[9,23] However, in approximately 20% of cells expressing mutant EGFP-STXBP1 (p.V84D, p.C180Y, p.M443R, and p.G544D), intense clusters of fluorescence signals were observed, likely representing protein aggregation.[9] The other 80% of cells showed a diffuse cytosolic protein distribution similar to that expressing the WT, but the signal intensity was much weaker, implying possible protein degradation. Protein degradation of mutant STXBP1 proteins was also confirmed by immunoblotting using an anti-Munc18 antibody[19] (Fig. 64–3C). These experiments suggested that mutant STXBP1 proteins would be aggregated or degraded in neurons, both leading to loss of STXBP1 function.

Degradation of *STXBP1* mRNA with Abnormal Splicing

The splicing, frameshift, and nonsense mutations would produce a premature stop codon; therefore, these mutant mRNAs are likely to be degraded by NMD.[24,25] In fact, NMD associated with abnormal splicing was demonstrated in lymphoblastoid cells derived from a patient harboring a c.663+5G>A mutation. Polymerase chain reaction (PCR) primers designed to amplify exons 7 to 10 amplified a single band (338 bp), corresponding to the WT *STXBP1* allele, using a cDNA template from a control lymphoblastoid cell lines (LCL; Fig. 64–3D). By contrast, a smaller band was detected from the patient's cDNA, in which exon 8 of *STXBP1* was skipped (Fig. 64–3D), resulting in the insertion of nine new amino

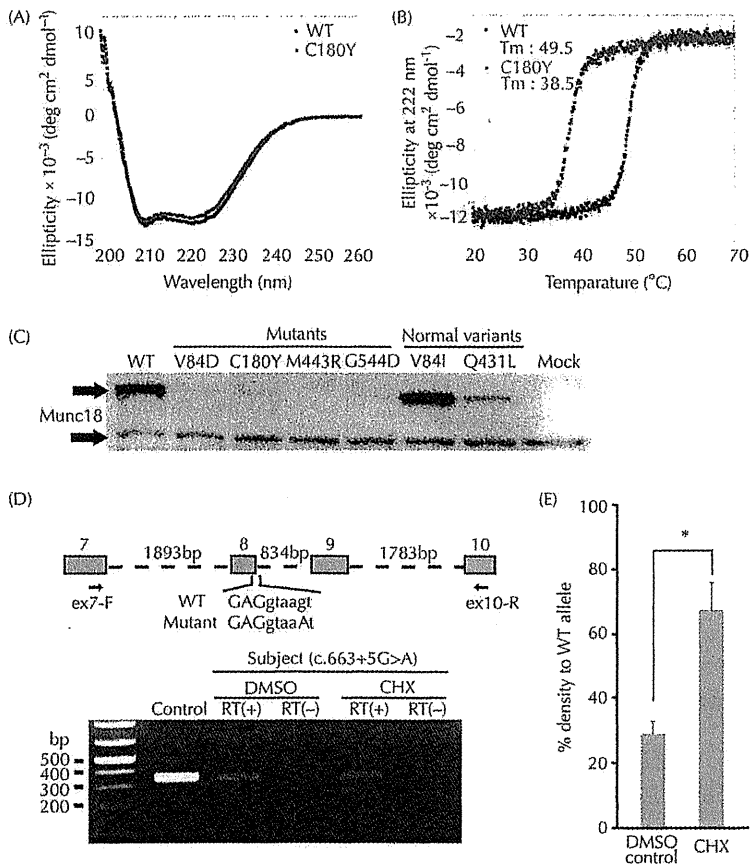

Figure 64–3. Characterization of mutant STXBP1 proteins and mRNAs with aberrant splicing. **A.** Circular dicroism spectra of the WT and C180Y-mutated STXBP1. The C180Y mutation is found to induce a subtle decrease in the helical contents of the STXBP1 structure by comparing the peaks of both proteins at 222 nm, where a large negative ellipticity value indicates a high helical content of the protein. **B.** Circular dicroic melting curves of the STXBP1 WT and C180Y proteins. Values of ellipticity at 222 nm are measured to monitor the thermal unfolding of the proteins. The C180Y mutant became unfolded at a lower temperature compared to the WT. Each dot represents the average of three repeated experiments, with standard deviations depicted as error bars. **C.** Immunoblot analysis of mutant STXBP1 proteins using a monoclonal anti-Munc18 antibody. Upper and lower bands represent EGFP-STXBP1 and endogenous STXBP1 proteins, respectively. Expression of four mutant STXBP1 proteins was not detected, while the WT and two normal variants could be detected. **D.** Top: Schematic representation of the genomic structure from exons 7 to 10 of *STXBP1*. Exons, introns, and primers are shown by boxes, dashed lines, and arrows, respectively. Sequences of exons and introns are presented in uppercase and lowercase, respectively. The mutation in intron 8 is highlighted in bold. Bottom: Reverse transcriptase-PCR analysis of patient 11 with a c.663+5G>A mutation and a normal control. Two PCR products were detected from the patient's cDNA: the upper one is the WT transcript and the lower one is the mutant. Only a single WT amplicon was detected in the control. The mutant amplicon was significantly increased by 30 μM cycloheximide (CHX) treatment compared to dimethyl sulfoxide (DMSO) treatment as a vehicle control. RT (+): with reverse transcriptase, RT (−): without reverse transcriptase as a negative control. **E.** Quantitative analysis of the NMD inhibition by CHX based on the data shown in **D.** $^{*}P = 0.0023$ by unpaired Student's *t*-test, two tailed. Averages of three repeated experiments are shown with error bars (s.d). Adapted from refs. 9 and 19.

acids followed by a premature stop codon at position 203. Moreover, the intensity ratio of the mutant compared to the normal band was increased by up to 67% after treatment with 30 μM cycloheximide, which inhibits NMD, compared to a ratio of 29% in the untreated condition (Fig. 64–3D,E). These facts suggest that the mutant mRNA possessing a premature stop codon suffered from degradation by NMD in neurons, resulting in haploinsufficiency.

Considering the degradation of STXBP1 proteins with missense mutations, NMD of mRNAs with premature stop codons and the effects of deletion of STXBP1, we conclude that haploinsufficiency of *STXBP1* causes OS.

HOW WOULD HAPLOINSUFFICIENCY OF *STXBP1* LEAD TO OS?

Impairment of Synaptic Vesicle Release

STXBP1 (*MUNC18-1*) is a member of the evolutionarily conserved Sec1/Munc-18 gene family that acts at specific steps of intracellular membrane transport.[26,27] In mammalian exocytosis, the vesicular SNARE protein, VAMP2 (also known as *synaptobrevin2*), and the target membrane SNARE proteins, Syntaxin-1 and SNAP25, constitute the core fusion machinery that bring two membranes into close apposition to fuse.[23,28] An *Stxbp1* null mutation led to complete loss of neurotransmitter secretion from synaptic vesicles throughout development in mice, though seizures have never been described.[16] Thus, *STXBP1* very likely plays a central role in synaptic vesicle release in coordination with SNARE proteins. The association of mutations of *STXBP1* with OS implies that perturbation of synaptic vesicle release forms part of the genetic basis of epilepsy. To date, the majority of genes associated with epilepsy syndromes are ion channel genes.[29] Synapsin I is a synaptic vesicle protein thought to regulate the kinetics of neurotransmitter release during priming of synaptic vesicles, and a mutation has been identified in a family with X-linked epilepsy and learning difficulties.[30] *STXBP1* is the second synaptic vesicle gene shown to be involved in epilepsy, and this finding will encourage further research into regulation of synaptic vesicle release and its involvement in seizures and related disorders.

Possible Interneuropathy

In *Stxbp1* heterozygous knockout mice, no seizures have been reported, and whole-cell recordings of autaptic glutamatergic or GABAergic (GABA: gamma-aminobutyric acid) neurons showed excitatory and inhibitory postsynaptic currents similar to those of WT littermate neurons upon single depolarizations.[31] However, with repeated stimulation, *Stxbp1*$^{+/-}$ neurons showed impaired synaptic function due to the reduced size and replenishment rate of readily releasable vesicles,[31] suggesting that heterozygous deletion of *Stxbp1* indeed affected synaptic function in mice. Interestingly, the reduction of readily releasable vesicles was more evident in GABAergic neurons than in glutamatergic neurons.[31] It has been reported that *Arx* is expressed in GABAergic interneurons and that *Arx* controls their genesis, migration, and differentiation, as *Arx* knockout mice showed a deficit of GABAergic interneurons.[32] Moreover, neuropathological examination of three patients with X-linked lissencephaly with absent corpus callosum and ambiguous genitalia, caused by *ARX* mutations, has suggested a loss of interneurons.[33] If haploinsufficiency of *STXBP1* affected GABAergic interneurons more severely than glutamatergic neurons in humans, as in mice, a defect in the GABAergic system could be postulated as a common pathophysiology among OS patients with *ARX* or *STXBP1* mutations. Ohtahara syndrome might be designated as a continuum of interneuronopathies.[34,35]

Cell Death of the Brainstem

As brain malformations are often associated with individuals with OS,[2,3] it could be speculated that *STXBP1* mutations would lead to abnormal brain structures directly related to the seizure phenotype of OS. However, we did not observe structural brain anomalies in any of the 14 OS patients with *STXBP1* defects. This is consistent with the findings that mice deleted for *Stxbp1* have normal brain architec-

ture. *Stxbp1* null mice, however, showed extensive cell death of mature neurons in lower brain areas, such as the brainstem; the lower brainstem was almost completely lost by embryonic day 18.[16] This is consistent with the suggestion that tonic seizures in OS might originate from subcortical structures, including the brainstem. Thus, in addition to the impaired synaptic vesicle release, it is possible that *STXBP1* haploinsufficiency leads to OS through microscopically impaired neuronal cell death in lower brain areas.

FUTURE CHALLENGES

Expansion of the Clinical Spectrum of *STXBP1* Mutations

Although OS is the core phenotype of *STXBP1* defects in our Japanese cohort (one-third of OS cases harbored *STXBP1* mutations), Hamdan et al. recently reported that two de novo *STXBP1* mutations, c.1162C>T (p.R388X) and c.169+1G>A, were identified in 2 out of 95 individuals with MR and nonsyndromic epilepsy.[36] According to their report, the two patients never showed the tonic seizures or infantile spasms associated with OS and WS, respectively. The onset of first seizures was at 6 weeks and 2 years of age, respectively. In addition, characteristic EEG patterns, such as suppression-burst or hypsarrhythmia, were never observed in these patients. Thus, the finding by Hamdan et al. indicated that *STXBP1* defects could cause a wide spectrum of clinical epileptic disorders in association with severe MR. Given that defects in synaptic dysfunction have also been implicated in many common neurodevelopmental disorders, such as MR, autism, and schizophrenia,[37,38] the possible involvement of *STXBP1* mutations in such common neurodevelopmental disorders is of interest. Elucidation of the molecular basis of synaptic vesicle processing disturbed by *STXBP1* mutations will allow us to understand not only the pathophysiology of infantile epilepsy, but also many neuropsychiatric conditions that present beyond childhood. The contribution of *STXBP1* mutations to EME also should be clarified, because myoclonic seizures, the characteristic feature of EME, are occasionally observed in 3/14 patients with *STXBP1* mutations.

Animal Model

An animal model is necessary to elucidate the pathophysiology of epilepsy caused by *STXBP1* mutations, including age dependency of seizure type and EEG pattern, and to test potential therapies directed specifically at OS and subsequent WS. The effect of gene dosage alterations of *STXBP1/Stxbp1* might vary between humans and mice: humans might be more susceptible than mice; thus, loss of function of one allele could cause seizures in humans but not in mice. Although it would be challenging to manipulate the gene dosage of *Stxbp1*—for example, in combination with a hypomorphic allele and a null allele—to the level at which mutant mice show a seizure phenotype, the establishment of an animal model will greatly benefit our understanding of the mechanisms of seizures in relation to impaired synaptic function.

DISCLOSURE STATEMENT

None of the authors have financial interests related to this work.

REFERENCES

1. Ohtahara S, Ishida T, Oka E, Yamatogi Y, Inoue H, Karita S, Ohtsuka Y. [On the specific age dependent epileptic syndrome: the early-infantile epileptic encephalopathy with suppression-burst.]. *No to Hattatsu*. 1976;8:270–279.
2. Djukic A, Lado FA, Shinnar S, Moshe SL. Are early myoclonic encephalopathy (EME) and the Ohtahara syndrome (EIEE) independent of each other? *Epilepsy Res*. 2006;70(suppl 1):S68–S76.
3. Ohtahara S, Yamatogi Y. Ohtahara syndrome: with special reference to its developmental aspects for differentiating from early myoclonic encephalopathy. *Epilepsy Res*. 2006;70(suppl 1):S58–S67.
4. Yamatogi Y, Ohtahara S. Early-infantile epileptic encephalopathy with suppression-bursts, Ohtahara syndrome; its overview referring to our 16 cases. *Brain Dev*. 2002;24:13–23.
5. Kato M, Saitoh S, Kamei A, Shiraishi H, Ueda Y, Akasaka M, Tohyama J, Akasaka N, Hayasaka K. A longer polyalanine expansion mutation in the ARX gene causes early infantile epileptic encephalopathy with suppression-burst pattern (Ohtahara syndrome). *Am J Hum Genet*. 2007;81:361–366.
6. Fullston T, Brueton L, Willis T, Philip S, MacPherson L, Finnis M, Gecz J, Morton J. Ohtahara syndrome in a family with an ARX protein truncation mutation (c.81C>G/p.Y27X). *Eur J Hum Genet*. 2010;18:157–162.
7. Absoud M, Parr JR, Halliday D, Pretorius P, Zaiwalla Z, Jayawant S. A novel ARX phenotype: rapid neurodegeneration with Ohtahara syndrome and a dyskinetic movement disorder. *Dev Med Child Neurol*. 2009;3:305–307.
8. Kato M, Koyama N, Ohta M, Miura K, Hayasaka K. Frameshift mutations of the ARX gene in familial Ohtahara syndrome. *Epilepsia*. 2010;51:1679–1684.
9. Saitsu H, Kato M, Mizuguchi T, Hamada K, Osaka H, Tohyama J, Uruno K, Kumada S, Nishiyama K, Nishimura A, Okada I, Yoshimura Y, Hirai S, Kumada T, Hayasaka K, Fukuda A, Ogata K, Matsumoto N. De novo mutations in the gene encoding STXBP1 (MUNC18-1) cause early infantile epileptic encephalopathy. *Nat Genet*. 2008;40:782–788.
10. Engel J Jr. Report of the ILAE classification core group. *Epilepsia*. 2006;47:1558–1568.
11. Molinari F, Raas-Rothschild A, Rio M, Fiermonte G, Encha-Razavi F, Palmieri L, Palmieri F, Ben-Neriah Z, Kadhom N, Vekemans M, Attie-Bitach T, Munnich A, Rustin P, Colleaux L. Impaired mitochondrial glutamate transport in autosomal recessive neonatal myoclonic epilepsy. *Am J Hum Genet*. 2005;76:334–339.
12. Molinari F, Kaminska A, Fiermonte G, Boddaert N, Raas-Rothschild A, Plouin P, Palmieri L, Brunelle F, Palmieri F, Dulac O, Munnich A, Colleaux L. Mutations in the mitochondrial glutamate carrier SLC25A22 in neonatal epileptic encephalopathy with suppression bursts. *Clin Genet*. 2009;76:188–194.
13. Kato M, Das S, Petras K, Sawaishi Y, Dobyns WB. Polyalanine expansion of ARX associated with cryptogenic West syndrome. *Neurology*. 2003;61:267–268.
14. Guerrini R, Moro F, Kato M, Barkovich AJ, Shiihara T, McShane MA, Hurst J, Loi M, Tohyama J, Norci V, Hayasaka K, Kang UJ, Das S, Dobyns WB. Expansion of the first PolyA tract of ARX causes infantile spasms and status dystonicus. *Neurology*. 2007;69:427–433.
15. Stromme P, Mangelsdorf ME, Shaw MA, Lower KM, Lewis SM, Bruyere H, Lutcherath V, Gedeon AK, Wallace RH, Scheffer IE, Turner G, Partington M, Frints SG, Fryns JP, Sutherland GR, Mulley JC, Gecz J. Mutations in the human ortholog of Aristaless cause X-linked mental retardation and epilepsy. *Nat Genet*. 2002;30:441–445.
16. Verhage M, Maia AS, Plomp JJ, Brussaard AB, Heeroma JH, Vermeer H, Toonen RF, Hammer RE, van den Berg TK, Missler M, Geuze HJ, Sudhof TC. Synaptic assembly of the brain in the absence of neurotransmitter secretion. *Science*. 2000;287:864–869.
17. Garcia EP, Gatti E, Butler M, Burton J, De Camilli P. A rat brain Sec1 homologue related to Rop and UNC18 interacts with syntaxin. *Proc Natl Acad Sci USA*. 1994;91:2003–2007.
18. Kalidas S, Santosh V, Shareef MM, Shankar SK, Christopher R, Shetty KT. Expression of p67 (Munc-18) in adult human brain and neuroectodermal tumors of human central nervous system. *Acta Neuropathol*. 2000;99:191–198.
19. Saitsu H, Kato M, Okada I, Kenji O, Higuchi T, Hoshino H, Kubota M, Arai H, Kimura S, Sudo A, Miyama S, Takami Y, Watanabe T, Nishimura A, Nishiyama K, Miyake N, Wada T, Osaka H, Kondo N, Hayasaka K, Matsumoto N. *STXBP1* mutations in early infantile epileptic encephalopathy with suppression-burst pattern. *Epilepsia*. 2010;51:2397–2405.
20. Kanazawa K, Kumada S, Kato M, Saitsu H, Kurihara E, Matsumoto N. Choreo-ballistic movements in a case carrying a missense mutation in syntaxin binding protein 1 gene. *Mov Disord*. 2010;25:2265–2267.
21. Dulubova I, Khvotchev M, Liu S, Huryeva I, Sudhof TC, Rizo J. Munc18-1 binds directly to the neuronal SNARE complex. *Proc Natl Acad Sci USA*. 2007;104:2697–2702.
22. Toonen RF, Verhage M. Munc18-1 in secretion: lonely Munc joins SNARE team and takes control. *Trends Neurosci*. 2007;30:564–572.
23. Rickman C, Medine CN, Bergmann A, Duncan RR. Functionally and spatially distinct modes of munc18-syntaxin 1 interaction. *J Biol Chem*. 2007;282:12097–12103.
24. Shyu AB, Wilkinson MF, van Hoof A. Messenger RNA regulation: to translate or to degrade. *EMBO J*. 2008;27:471–481.
25. Maquat LE, Kinniburgh AJ, Rachmilewitz EA, Ross J. Unstable beta-globin mRNA in mRNA-deficient β° thalassemia. Cell. 1981;27:543–553.
26. Sudhof TC. The synaptic vesicle cycle. *Annu Rev Neurosci*. 2004;27:509–547.
27. Weimer RM, Richmond JE. Synaptic vesicle docking: a putative role for the Munc18/Sec1 protein family. *Curr Top Dev Biol*. 2005;65:83–113.
28. Rizo J, Rosenmund C. Synaptic vesicle fusion. *Nat Struct Mol Biol*. 2008;15:665–674.
29. Gurnett CA, Hedera P. New ideas in epilepsy genetics: novel epilepsy genes, copy number alterations, and gene regulation. *Arch Neurol*. 2007;64:324–328.
30. Garcia CC, Blair HJ, Seager M, Coulthard A, Tennant S, Buddles M, Curtis A, Goodship JA. Identification of a mutation in synapsin I, a synaptic vesicle protein, in a family with epilepsy. *J Med Genet*. 2004;41:183–186.
31. Toonen RF, Wierda K, Sons MS, de Wit H, Cornelisse LN, Brussaard A, Plomp JJ, Verhage M. Munc18-1 expression levels control synapse recovery by regulating readily releasable pool size. *Proc Natl Acad Sci USA*. 2006;103:18332–18337.
32. Kitamura K, Yanazawa M, Sugiyama N, Miura H, Iizuka-Kogo A, Kusaka M, Omichi K, Suzuki R, Kato-Fukui Y, Kamiirisa K, Matsuo M, Kamijo S, Kasahara M, Yoshioka H, Ogata T, Fukuda T, Kondo I, Kato M, Dobyns WB, Yokoyama M, Morohashi K. Mutation of ARX causes abnormal development of forebrain and testes in mice and X-linked lissencephaly with abnormal genitalia in humans. *Nat Genet*. 2002;32:359–369.
33. Bonneau D, Toutain A, Laquerriere A, Marret S, Saugier-Veber P, Barthez MA, Radi S, Biran-Mucignat V, Rodriguez D, Gelot A. X-linked lissencephaly with absent corpus callosum and ambiguous genitalia (XLAG): clinical, magnetic resonance imaging, and neuropathological findings. *Ann Neurol*. 2002;51:340–349.
34. Kato M. A new paradigm for West syndrome based on molecular and cell biology. *Epilepsy Res*. 2006;70(suppl 1):S87–S95.
35. Kato M, Dobyns WB. X-linked lissencephaly with abnormal genitalia as a tangential migration disorder causing intractable epilepsy: proposal for

a new term, "interneuronopathy." *J Child Neurol.* 2005;20:392–397.
36. Hamdan FF, Piton A, Gauthier J, Lortie A, Dubeau F, Dobrzeniecka S, Spiegelman D, Noreau A, Pellerin S, Cote M, Henrion E, Fombonne E, Mottron L, Marineau C, Drapeau P, Lafreniere RG, Lacaille JC, Rouleau GA, Michaud JL. De novo STXBP1 mutations in mental retardation and nonsyndromic epilepsy. *Ann Neurol.* 2009;65:748–753.
37. Guilmatre A, Dubourg C, Mosca AL, Legallic S, Goldenberg A, Drouin-Garraud V, Layet V, Rosier A, Briault S, Bonnet-Brilhault F, Laumonnier F, Odent S, Le Vacon G, Joly-Helas G, David V, Bendavid C, Pinoit JM, Henry C, Impallomeni C, Germano E, Tortorella G, Di Rosa G, Barthelemy C, Andres C, Faivre L, Frebourg T, Saugier Veber P, Campion D. Recurrent rearrangements in synaptic and neurodevelopmental genes and shared biologic pathways in schizophrenia, autism, and mental retardation. *Arch Gen Psychiatry.* 2009;66:947–956.
38. Ramocki MB, Zoghbi HY. Failure of neuronal homeostasis results in common neuropsychiatric phenotypes. *Nature.* 2008;455:912–918.

Chapter 65

mTOR and Epileptogenesis in Developmental Brain Malformations

Michael Wong
Peter B. Crino

INTRODUCTION

Malformations of cortical development (MCDs) are among the most common causes of epilepsy. While a wide variety of types and classifications of MCDs exists,[1] a subset of focal cortical malformations (FCMs), including tuberous sclerosis complex (TSC), focal cortical dysplasia, ganglioglioma, and hemimegalencephaly, is associated with an especially high incidence of epilepsy and other neurological deficits, such as cognitive dysfunction and autism.[2,3] Epilepsy related to these focal developmental brain malformations is often refractory to medical therapy. Even in patients whose seizures are well controlled with medications, currently available drugs are only symptomatic treatments that help suppress seizures; they have not been demonstrated to have antiepileptogenic or disease-modifying properties in preventing or altering the long-term prognosis of epilepsy. Although epilepsy surgery may eliminate seizures in some medically intractable cases, many patients are not good candidates for surgery or continue to have seizures despite surgical intervention. Thus, novel therapeutic strategies are needed to reduce the burden of seizures and other neurological symptoms caused by MCDs or, ideally, to prevent the development of epilepsy in the first place.

Tuberous sclerosis complex (TSC) is often viewed as a prototypical FCM associated with epilepsy, providing a detailed understanding of the clinical features, the pathological substrates, and now the molecular-genetic pathophysiology of this disease.[4,5] Up to 90% of patients with TSC have epilepsy, most of whom are refractory to seizure medications.[6] The cortical tuber is the pathological hallmark of TSC and is strongly correlated with the neurological manifestations including seizures, cognitive disability, and autism. Cortical tubers are characterized by a focal loss of normal cortical organization or lamination and the presence of a spectrum of abnormal dysmorphic or cytomegalic cell types. Although the mechanisms causing epilepsy in TSC are incompletely understood, a number of cellular and molecular abnormalities have been identified in both tuber and peri-tuber tissue from TSC patients that likely promote epileptogenesis and other neurological deficits in TSC, such as molecular

REPORT

De Novo and Inherited Mutations in *COL4A2*, Encoding the Type IV Collagen α2 Chain Cause Porencephaly

Yuriko Yoneda,[1] Kazuhiro Haginoya,[2,3] Hiroshi Arai,[4] Shigeo Yamaoka,[5] Yoshinori Tsurusaki,[1] Hiroshi Doi,[1] Noriko Miyake,[1] Kenji Yokochi,[6] Hitoshi Osaka,[7] Mitsuhiro Kato,[8] Naomichi Matsumoto,[1] and Hirotomo Saitsu[1,*]

Porencephaly is a neurological disorder characterized by fluid-filled cysts or cavities in the brain that often cause hemiplegia. It has been suggested that porencephalic cavities result from focal cerebral degeneration involving hemorrhages. De novo or inherited heterozygous mutations in *COL4A1*, which encodes the type IV α1 collagen chain that is essential for structural integrity for vascular basement membranes, have been reported in individuals with porencephaly. Most mutations occurred at conserved Gly residues in the Gly-Xaa-Yaa repeats of the triple-helical domain, leading to alterations of the α1α1α2 heterotrimers. Here we report on two individuals with porencephaly caused by a heterozygous missense mutation in *COL4A2*, which encodes the type IV α2 collagen chain. Mutations c.3455G>A and c.3110G>A, one in each of the individuals, cause Gly residues in the Gly-Xaa-Yaa repeat to be substituted as p.Gly1152Asp and p.Gly1037Glu, respectively, probably resulting in alterations of the α1α1α2 heterotrimers. The c.3455G>A mutation was found in the proband's mother, who showed very mild monoparesis of the left upper extremity, and the maternal elder uncle, who had congenital hemiplegia. The maternal grandfather harboring the mutation is asymptomatic. The c.3110G>A mutation occurred de novo. Our study confirmed that abnormalities of the α1α1α2 heterotrimers of type IV collagen cause porencephaly and stresses the importance of screening for *COL4A2* as well as for *COL4A1*.

Porencephaly (MIM 175780) is a neurological disorder characterized by fluid-filled cysts or cavities in the brain.[1] It has been suggested that porencephalic cysts are caused by a disturbance of vascular supply leading to cerebral degeneration.[2,3] Porencephaly clinically causes hemiplegia (most often), tetraplegia, epilepsy, and intellectual disability.[4,5] Monozygous twinning, maternal cardiac arrest or abdominal trauma, a deficient protein C anticoagulant pathway, or cytomegalovirus infections are risk factors for sporadic porencephaly.[2,6] Recently, mutations in the gene encoding type IV collagen α1 chain (*COL4A1* [MIM 120130]) have been shown to cause familial porencephaly.[7] Since then, de novo and inherited *COL4A1* mutations have been reported,[8–10] confirming that *COL4A1* abnormalities are involved in both sporadic and familial porencephaly. Type IV collagens are basement membrane proteins that are expressed in all tissues including the vasculature. COL4A1 (α1 chain) and COL4A2 (α2 chain) are the most abundant type IV collagens, and form heterotrimers with 2:1 stoichiometry (α1α1α2).[11] A mouse model of the heterozygous *COL4A1* mutation (*Col4a1*$^{+/\Delta ex40}$) showed cerebral hemorrhage and porencephaly and displayed abnormalities of vascular basement membranes, such as uneven edges, inconsistent density, and highly variable thickness.[7] In addition, a dominant negative effect of the *Col4a1*$^{+/\Delta ex40}$ mutation was demonstrated on collagen IV α1α1α2 heterotrimer assembly and its secretion.[7] In humans, most mutations are substitutions of the conserved Gly residue in the Gly-Xaa-Yaa repeat of the triple-helical domain, and they have a dominant negative effect on heterotrimer formation.[11,12]

COL4A2 (MIM 120090), which encodes the type IV α2 collagen chain, is a possible candidate for porencephaly because its mutations may affect the α1α1α2 heterotrimer. Supporting this idea, osteogenesis imperfecta type I-IV (MIM 166200, 166210, 259420, and 166220), which is characterized by abnormal bone fragility and low bone mass, is caused by mutations in both *COL1A1* (MIM 120150) and *COL1A2* (MIM 120160) that may interfere with formation of the collagen I α1α1α2 heterotrimer.[13] Moreover, mice lines harboring *Col4a2* point mutations (*Col4a2*^{ENU415}, c.227G>T [p.Val31Phe]; *Col4a2*^{ENU4003} and *Col4a2*^{ENU4020}, c.2073G>A [p.Gly646Asp]) showed abnormalities of the lens, cornea, and vascular stability.[14] In the brains of the mutants, pseudocysts in the upper cortical plate, hemorrhages surrounding small blood vessels, and focal hemorrhagic necroses were observed, indicating that *Col4a2* mutations cause abnormalities of the cerebral vasculature similar to those caused by *Col4a1* mutations.[7,14] In this study, we screened for *COL4A2* mutations in 35 Japanese individuals with porencephaly. Substitutions of a Gly residue in the Gly-Xaa-Yaa repeat were identified in two individuals (individuals 1 and 2). Clinical information and peripheral blood samples were

[1]Department of Human Genetics, Yokohama City University Graduate School of Medicine, Fukuura 3-9, Kanazawa-ku, Yokohama 236-0004, Japan; [2]Department of Pediatrics, Tohoku University School of Medicine, Seiryo-machi 1-1, Aoba-ku, Sendai 980-8574, Japan; [3]Department of Pediatric Neurology, Takuto Rehabilitation Center for Children, Akiu-machi 20, Taihaku-ku, Sendai 982-0241, Japan; [4]Department of Pediatric Neurology, Morinomiya Hospital, Morinomiya2-1-88, Joto-ku, Osaka 536-0025, Japan; [5]Department of Neonatal Medicine and Pediatrics, Osaka Medical College, 2-7 Daigakumachi, Takatsuki, Osaka 569-8686, Japan; [6]Department of Pediatric Neurology, Seirei-Mikatahara General Hospital, 2-12-12 Sumiyoshi, Naka-ku, Hamamatsu 430-8558, Japan; [7]Division of Neurology, Clinical Research Institute, Kanagawa Children's Medical Center, 2-138-4 Mutsukawa, Minami-ku, Yokohama 232-8555, Japan; [8]Department of Pediatrics, Yamagata University School of Medicine, Iida-nishi 2-2-2, Yamagata 990-9585, Japan
*Correspondence: hsaitsu@yokohama-cu.ac.jp
DOI 10.1016/j.ajhg.2011.11.016. ©2012 by The American Society of Human Genetics. All rights reserved.

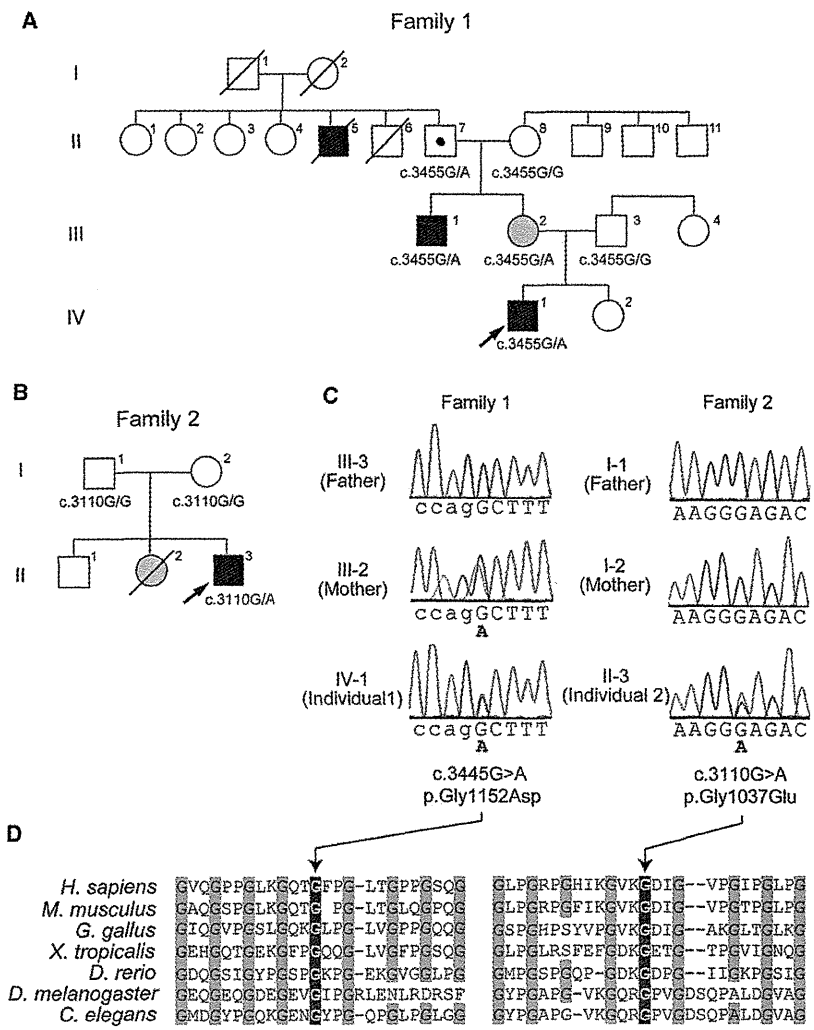

Figure 1. Pedigrees and *COL4A2* Mutations in Individuals 1 and 2

Pedigrees of family 1(A) and family 2 (B). The arrows indicate the probands (Individual 1 in family 1 and individual 2 in family 2). The segregation of the *COL4A2* mutations is shown. In family 1, the proband's mother (III-2) and maternal uncle (III-1) had mild monoparesis of the left upper extremity and congenital left hemiplegia and an assisted walk, respectively. The maternal grandfather (II-7) was healthy. The elder granduncle (II-5) was also afflicted by congenital hemiplegia and died in his 60s. (B) In family 2, the proband had a heterozygous mutation, but his parents did not have this mutation, indicating that the mutation occurred de novo. His elder sister (II-2) had intraventricular hemorrhage two days after birth but her DNA was unavailable.

(C) Electropherogram of family 1 (left) and family 2 (right). The intron and exon bases are in lower and upper cases, respectively. The c.3455G>A (p.Gly1152Asp) mutation in individual 1 was inherited from his mother. The c.3110G>A (p.Gly1037Glu) mutation in individual 2 occurred de novo.

(D) Multiple amino acid sequence alignments of COL4A2 proteins showing the evolutionarily conserved amino acids. The protein sequences obtained from the National Center for Biotechnology Information protein database are, NP_001837.2 (*Homo sapiens*), NP_034062.3 (*Mus musculus*), NP_001155862.1 (*Gallus gallus*), XP_002933063.1 (*Xenopus tropicalis*), XP_687811.5 (*Danio rerio*), AAB64082.1 (*Drosophila melanogaster*), and CAA80537.1 (*Caenorhabditis elegans*). The multiple sequence alignment was performed via the CLUSTALW website (see Web Resources). The positions of the conserved Gly residues in the Gly-X-Y repeats where the mutations occurred are highlighted with gray.

obtained from their family members after obtaining written informed consent. Experimental protocols were approved by the Institutional Review Board of Yokohama City University School of Medicine.

Individual 1 is 7 years old and a product of nonconsanguineous healthy parents (Figure 1A, arrow). There was no abdominal traumatism associated with the pregnancy and delivery in the mother. The individual was born at 36 weeks' gestation with a planned Caesarean section because, at 31 weeks' gestation, an antenatal ultrasound scan revealed an enlarged right lateral ventricle. Apgar scores were 9 at 1 min and 10 at 5 min. He weighed 2,900 g (+1.09 standard deviation [SD]) and had a head circumference of 32.5 cm (+0.05 SD). His early development was delayed with poor left hand use and abnormal leg movement. Brain magnetic resonance imaging (MRI) at 6 months showed an enlarged right lateral ventricle. Abrupt vomiting and nausea followed by motionless arrest developed at the 10 months. An electroencephalogram (EEG) showed focal spikes in the right frontal region, and carbamazepine treatment was initiated at the 12 months. Rehabilitation was started at 10 months. The individual started rolling at 12 months, crawling at 18 months, and walking alone at 3 years. He had spastic triplegia (diplegia and left hemiplegia) showing hemiplegic and diplegic gait with fluent speech and normal word comprehension. At the 5 years of age, he underwent orthopedic surgery for foot deformity due to spastic paresis. An EEG showed spikes in the right occipital to posterior temporal region and midcentral region. A brain MRI at age 6 showed an enlarged right lateral ventricle, reduced volume of the right frontal white matter, and atrophic right cerebral peduncle and body of corpus callosum (Figures 2A–2C). His intelligent quotient [IQ] score, evaluated at 6 years with Wechsler Intelligence Scale for Children-Third Edition (WISC-III), was 74 (his performance IQ was 69 and his verbal IQ was

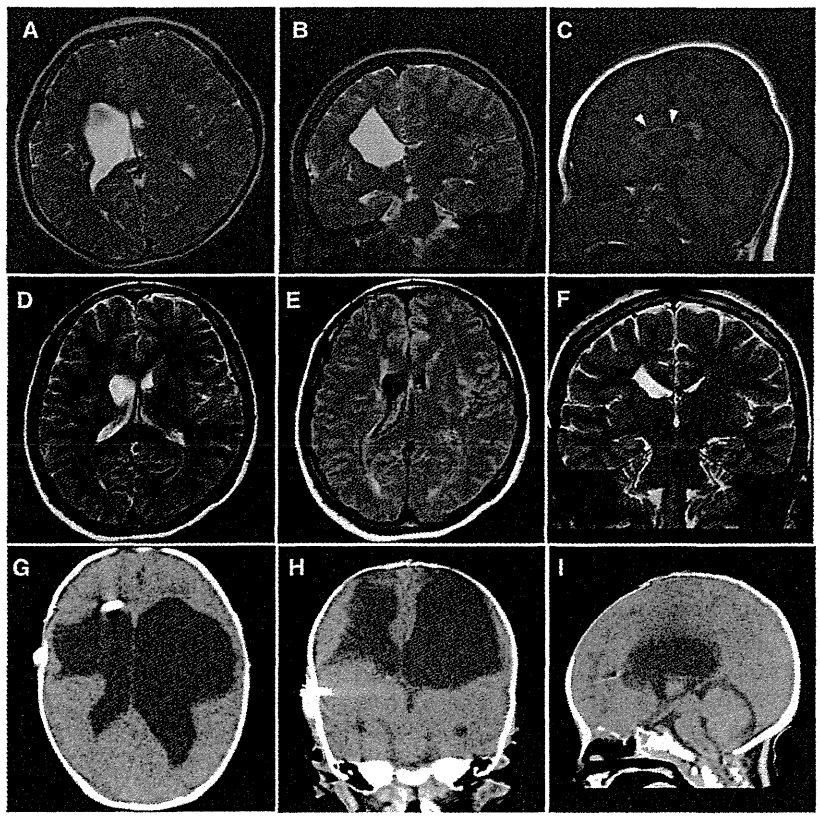

Figure 2. Brain Imaging in Individuals 1 and 2

(A–C) Brain MRIs of individual 1 at 6 years old; (A) T2-weighted axial image. (B) Coronal image. The images in (A) and (B) show an enlarged right lateral ventricle and a reduced volume of the right frontal white matter. (C) T1-weighted midline sagittal image showing atrophy of the body of the corpus callosum (arrowheads). The lesion responsible for the left leg paresis is not evident in these images.

(D–F) Brain MRIs of individual 1's mother at age 31. (D) T2-weighted axial and (F) coronal images show a mildly enlarged right lateral ventricle. (E) FLAIR axial image shows high signal intensity around the enlarged ventricular wall, which is consistent with mild porencephaly or periventricular venous infarction.

(G–I) CT images of individual 2 at 2 months of age. (G) Axial image. (H) Coronal image. (I) Sagittal image. The images in (G), (H), and (I) show an enlarged bilateral lateral ventricle and an extremely reduced volume of bilateral frontal white matter. The V-P shunt tube is also visible in the right lateral ventricle. The pontocerebellar structures seem to be normal.

82). The individual is now 7 years old and attending a local school. He can walk with ankle foot orthosis and hand assist. The epilepsy is well controlled with carbamazepine and clobazam. He does not show hematuria, muscular cramps, or ophthalmic abnormalities. His mother was born at term without asphyxia after an uneventful pregnancy. She had convulsions at the age of 18 months, and anticonvulsant was started under a diagnosis of focal epilepsy. Seizures were well controlled and treatment was discontinued at the age of 13. She first realized clumsiness of the left hand when she started learning piano and recorder at the age of 9. When she was a junior high school student, she felt severe headaches, and abnormal findings were pointed out in the brain MRI study (detailed information was unavailable). However, she did not undergo any more examinations because the headaches disappeared and did not recur. Neurological examination at 31 years revealed very mild monoparesis of the left upper extremity. She had neither spasticity nor exaggerated tendon reflexes. The grip power of her right and left hands was 25 and 15 kg, respectively. Mirror movement was observed on the right hand. The brain MRI revealed a mildly enlarged right lateral ventricle and high signal intensity around the enlarged ventricular wall on a Fluid Attenuated Inversion Recovery (FLAIR) image, which is consistent with mild porencephaly or periventricular venous infarction (Figures 2D–2F). MR angiography showed no aneurysms. Of note, his maternal elder uncle also showed congenital left hemiplegia with an assisted walk, and his maternal granduncle had also been afflicted by congenital hemiplegia, suggesting a genetic predisposition in the family (Figure 1A).

Individual 2 is 1 year and 4 months old and a product of nonconsanguineous healthy parents (Figure 1B, arrow). There was no abdominal traumatism associated with the pregnancy and delivery in the mother. He was born at 35 weeks' gestation. His birth weight was 1,694 g (−2.36 SD) and his head circumference was 29 cm (−1.77 SD). Mild asphyxia was observed, and he had Apgar scores of 3 at 1 min and 7 at 5 min. An ultrasound scan at 6 hr after birth revealed a parenchymal hemorrhage of the right cerebral hemisphere with an enlarged left lateral ventricle. Because a blood test revealed significant increases in prothrombin time (29.3 s) and activated partial thromboplastin time (104.3 s), but not in D-dimer (0.7 μg/ml) at 1 day after birth, he was treated with a daily infusion of fresh frozen plasma for 12 days. At 37 days after birth, he underwent a ventricular-peritoneal shunt (V-P shunt) operation for progressive enlargement of the lateral ventricle. Computed tomography (CT) at 2 months of age showed an enlarged bilateral lateral ventricle and an extremely reduced volume of bilateral frontal white matter (Figures 2G–2I). Blood coagulation was normalized at 7 months. At the 7 months, the individual did not show any head control or rolling, and presented with abnormal posturing and spastic quadriplegia dominant on the left side of his body. With

rehabilitation, he had full-range visual pursuit, a social smile, and incomplete head control. Although his spasticity improved, exaggerated deep tendon reflexes with synergic voluntary movement of the distal part of the extremities were recognized. An EEG at 1 year of age showed no epileptic discharges. His present developmental quotient is below 20. He did not show hematuria, muscular cramps, intracranial aneurysms, or cataracts. His elder sister was found to have an intraventricular hemorrhage two days after birth and underwent a V-P shunt. Her development was almost normal, and internal strabismus was noted. Unfortunately, she died in an accident at the age of four, and so her DNA was unavailable (Figure 1B).

Genomic DNA was isolated from peripheral blood leukocytes according to standard methods. DNA for mutation screening was amplified by illustra GenomiPhi V2 DNA Amplification Kit (GE Healthcare, Buckinghamshire, UK). The DNA of family members of individual 1 was isolated from saliva samples with Oragene (DNA Genotek Inc., Ontario, Canada). Exons 2 to 48 covering the entire *COL4A2* coding region (GenBank accession number NM_001846.2) were examined by high-resolution melting curve (HRM) analysis or directly sequenced (for exon 46). The samples showing an aberrant melting curve pattern in the HRM analysis were sequenced. PCR primers and conditions are shown in Table S1, available online. All the mutations were verified with genomic DNA as a template. Two heterozygous mutations, c.3455G>A (p.Gly1152Asp) in individual 1 and c.3110G>A (p.Gly1037Glu) in individual 2, were identified. Both mutations occur at evolutionary conserved Gly residues in the Gly-X-Y repeats (Figure 1D), suggesting that the two mutations may alter the collagen IV $\alpha1\alpha1\alpha2$ heterotrimers. These mutations were absent in 200 normal Japanese controls, and our evaluation with web-based prediction tools strongly suggested that these substitutions are pathogenic (Table S2). Screening for *COL4A1* mutations was negative for both individuals (data not shown). The c.3455G>A mutation was found in the proband's mother and the maternal uncle, who showed very mild monoparesis of the left upper extremity and congenital left hemiplegia, respectively, and in maternal grandfather who is asymptomatic (Figures 1A and 1B). Therefore the c.3455G>A mutation can be considered as a pathogenic mutation with incomplete penetrance. The c.3110G>A mutation in individual 2 was not found in his parents, indicating that this mutation occurred de novo (Figure 1C).

Here we report two individuals with porencephaly who harbor *COL4A2* mutations. In individual 2, the mutation occurred de novo. It is noteworthy that individual 2's elder sister also suffered from an intraventricular hemorrhage. A coincidental phenocopy in the sister is possible and would be consistent with de novo occurrence of the mutation. Alternatively, the sister might have the same mutation, which could be inherited from either one of the parents with a germline-mosaic mutation, though it was impossible to examine the sister because her sample is unavailable. Thus, with the present data, we concluded that the c.3110G>A mutation occurred de novo. On the other hand, the mutation in individual 1 was inherited from his mildly affected mother. In addition, congenital hemiplegia is observed in familial members of individual 1; the segregation of the c.3455G>A mutation is consistent with a dominant trait with incomplete penetrance. Such incomplete penetrance also has been reported in familial porencephalies with *COL4A1* mutations,[8,9] suggesting that abnormalities of collagen IV $\alpha1\alpha1\alpha2$ heterotrimers may conspire with other risk factors. The porencephalic cyst was unilateral in individual 1 and bilateral in individual 2, who required shunting, indicating variable severities caused by the different *COL4A2* mutations. Most porencephalic cysts caused by *COL4A1* mutations are unilateral;[9] however, Meuwissen et al. recently reported *de novo COL4A1* mutations in sporadic extensive bilateral porencephaly resembling hydranencephaly, indicating similar variable severities caused by *COL4A1* mutations.[10] Thus the involvement of *COL4A1* and *COL4A2* abnormalities should be considered in porencephaly and related pre- and perinatal cerebral hemorrhages, regardless of their severities.

It has been reported that *COL4A1* mutations cause a variety of phenotypes, including porencephaly, infantile hemiplegia, and cerebral small vessel diseases involving both ischemic stroke and intracerebral hemorrhage with radiological features of lacunar infarction, and leukoaraiosis in adult individuals.[9,15–18] The phenotypes in the central nervous system are often accompanied by ocular features (cataracts, retinal vessel tortuosity and hemorrhage, and defects of the anterior segment of the eye), nephropathy, and muscle cramps.[9,16,17] Considering the common pathological mechanism between *COL4A1* and *COL4A2* mutations (abnormalities of collagen IV $\alpha1\alpha1\alpha2$ heterotrimers), *COL4A2* mutations also may be involved in small vessel diseases that can be manifested in adulthood. Supporting this idea, mice lines harboring *Col4A2* point mutations showed cataracts, abnormalities of the lens and the cornea, and cerebral abnormalities.[14] Thus it is important to identify mutations in both *COL4A1* and *COL4A2* in individuals with porencephaly as well as in asymptomatic carriers, for whom the prevention of stroke and genetic counseling are quite important. Identification of pathogenic mutations in individuals with porencephaly is of great interest for obstetricians and pediatricians, and for neurologists working for adult individuals.

In summary, we have identified mutations in *COL4A2* as a genetic cause of both sporadic and familial porencephaly. Our data further support the importance of genetic testing in porencephaly and related pre- and perinatal cerebral hemorrhages for which the genetic predisposition is gradually being uncovered.

Supplemental Data

Supplemental Data include two tables and can be found with this article online at http://www.cell.com/AJHG/.

Acknowledgments

We would like to thank all the individuals and their families for their participation in this study. This work was supported by research grants from the Ministry of Health, Labour and Welfare (K.H., N. Miyake, H.O., M.K., N. Matsumoto, and H.S.), the Japan Science and Technology Agency (N. Matsumoto), the Strategic Research Program for Brain Sciences (N. Matsumoto), and a Grant-in-Aid for Scientific Research on Innovative Areas-(Foundation of Synapse and Neurocircuit Pathology)-from the Ministry of Education, Culture, Sports, Science and Technology of Japan (N. Matsumoto), a Grant-in-Aid for Scientific Research from Japan Society for the Promotion of Science (H.O., N. Matsumoto), a Grant-in-Aid for Young Scientist from Japan Society for the Promotion of Science (H.D., N. Miyake, H.S.) and a grant from the Takeda Science Foundation (N. Miyake and N. Matsumoto). This work has been done at the Advanced Medical Research Center, Yokohama City University, Japan.

Received: September 27, 2011
Revised: November 4, 2011
Accepted: November 17, 2011
Published online: December 29, 2011

Web Resources

The URLs for data presented herein are as follows:

Clustal W, http://www.genome.jp/tools/clustalw/
GenBank, http://www.ncbi.nlm.nih.gov/Genbank/
Online Mendelian Inheritance in Man (OMIM), http://www.omim.org

References

1. Berg, R.A., Aleck, K.A., and Kaplan, A.M. (1983). Familial porencephaly. Arch. Neurol. *40*, 567–569.
2. Govaert, P. (2009). Prenatal stroke. Semin. Fetal Neonatal Med. *14*, 250–266.
3. Hunter, A. (2006). Porencephaly. In Human Malformations and related Anomalies, S. Re and H. Jg, eds. (New York: Oxford University Press), pp. 645–654.
4. Mancini, G.M., de Coo, I.F., Lequin, M.H., and Arts, W.F. (2004). Hereditary porencephaly: clinical and MRI findings in two Dutch families. Eur. J. Paediatr. Neurol. *8*, 45–54.
5. Vilain, C., Van Regemorter, N., Verloes, A., David, P., and Van Bogaert, P. (2002). Neuroimaging fails to identify asymptomatic carriers of familial porencephaly. Am. J. Med. Genet. *112*, 198–202.
6. Moinuddin, A., McKinstry, R.C., Martin, K.A., and Neil, J.J. (2003). Intracranial hemorrhage progressing to porencephaly as a result of congenitally acquired cytomegalovirus infection—an illustrative report. Prenat. Diagn. *23*, 797–800.
7. Gould, D.B., Phalan, F.C., Breedveld, G.J., van Mil, S.E., Smith, R.S., Schimenti, J.C., Aguglia, U., van der Knaap, M.S., Heutink, P., and John, S.W. (2005). Mutations in *Col4a1* cause perinatal cerebral hemorrhage and porencephaly. Science *308*, 1167–1171.
8. Breedveld, G., de Coo, I.F., Lequin, M.H., Arts, W.F., Heutink, P., Gould, D.B., John, S.W., Oostra, B., and Mancini, G.M. (2006). Novel mutations in three families confirm a major role of *COL4A1* in hereditary porencephaly. J. Med. Genet. *43*, 490–495.
9. Lanfranconi, S., and Markus, H.S. (2010). *COL4A1* mutations as a monogenic cause of cerebral small vessel disease: a systematic review. Stroke *41*, e513–e518.
10. Meuwissen, M.E., de Vries, L.S., Verbeek, H.A., Lequin, M.H., Govaert, P.P., Schot, R., Cowan, F.M., Hennekam, R., Rizzu, P., Verheijen, F.W., et al. (2011). Sporadic *COL4A1* mutations with extensive prenatal porencephaly resembling hydranencephaly. Neurology *76*, 844–846.
11. Khoshnoodi, J., Pedchenko, V., and Hudson, B.G. (2008). Mammalian collagen IV. Microsc. Res. Tech. *71*, 357–370.
12. Engel, J., and Prockop, D.J. (1991). The zipper-like folding of collagen triple helices and the effects of mutations that disrupt the zipper. Annu. Rev. Biophys. Biophys. Chem. *20*, 137–152.
13. Gajko-Galicka, A. (2002). Mutations in type I collagen genes resulting in osteogenesis imperfecta in humans. Acta Biochim. Pol. *49*, 433–441.
14. Favor, J., Gloeckner, C.J., Janik, D., Klempt, M., Neuhäuser-Klaus, A., Pretsch, W., Schmahl, W., and Quintanilla-Fend, L. (2007). Type IV procollagen missense mutations associated with defects of the eye, vascular stability, the brain, kidney function and embryonic or postnatal viability in the mouse, Mus musculus: an extension of the *Col4a1* allelic series and the identification of the first two *Col4a2* mutant alleles. Genetics *175*, 725–736.
15. Vahedi, K., and Alamowitch, S. (2011). Clinical spectrum of type IV collagen (COL4A1) mutations: a novel genetic multisystem disease. Curr. Opin. Neurol. *24*, 63–68.
16. Sibon, I., Coupry, I., Menegon, P., Bouchet, J.P., Gorry, P., Burgelin, I., Calvas, P., Orignac, I., Dousset, V., Lacombe, D., et al. (2007). *COL4A1* mutation in Axenfeld-Rieger anomaly with leukoencephalopathy and stroke. Ann. Neurol. *62*, 177–184.
17. Alamowitch, S., Plaisier, E., Favrole, P., Prost, C., Chen, Z., Van Agtmael, T., Marro, B., and Ronco, P. (2009). Cerebrovascular disease related to *COL4A1* mutations in HANAC syndrome. Neurology *73*, 1873–1882.
18. Gould, D.B., Phalan, F.C., van Mil, S.E., Sundberg, J.P., Vahedi, K., Massin, P., Bousser, M.G., Heutink, P., Miner, J.H., Tournier-Lasserve, E., and John, S.W. (2006). Role of COL4A1 in small-vessel disease and hemorrhagic stroke. N. Engl. J. Med. *354*, 1489–1496.

Journal of Human Genetics (2012) 57, 197–201
© 2012 The Japan Society of Human Genetics All rights reserved 1434-5161/12 $32.00
www.nature.com/jhg

ORIGINAL ARTICLE

A family of oculofaciocardiodental syndrome (OFCD) with a novel *BCOR* mutation and genomic rearrangements involving *NHS*

Yukiko Kondo[1], Hirotomo Saitsu[1], Toshinobu Miyamoto[2], Kiyomi Nishiyama[1], Yoshinori Tsurusaki[1], Hiroshi Doi[1], Noriko Miyake[1], Na-Kyung Ryoo[3], Jeong Hun Kim[3], Young Suk Yu[3] and Naomichi Matsumoto[1]

Oculofaciocardiodental syndrome (OFCD) is an X-linked dominant disorder associated with male lethality, presenting with congenital cataract, dysmorphic face, dental abnormalities and septal heart defects. Mutations in *BCOR* (encoding BCL-6-interacting corepressor) cause OFCD. Here, we report on a Korean family with common features of OFCD including bilateral 2nd–3rd toe syndactyly and septal heart defects in three affected females (mother and two daughters). Through the mutation screening and copy number analysis using genomic microarray, we identified a novel heterozygous mutation, c.888delG, in the *BCOR* gene and two interstitial microduplications at Xp22.2–22.13 and Xp21.3 in all the three affected females. The *BCOR* mutation may lead to a premature stop codon (p.N297IfsX80). The duplication at Xp22.2–22.13 involved the *NHS* gene causative for Nance–Horan syndrome, which is an X-linked disorder showing similar clinical features with OFCD in affected males, and in carrier females with milder presentation. Considering the presence of bilateral 2nd–3rd toe syndactyly and septal heart defects, which is unique to OFCD, the mutation in *BCOR* is likely to be the major determinant for the phenotypes in this family.
Journal of Human Genetics (2012) **57,** 197–201; doi:10.1038/jhg.2012.4; published online 2 February 2012

Keywords: *BCOR*; congenital cataract; frameshift mutation; genomic rearrangement; Nance-Horan syndrome; *NHS*; oculofaciocardiodental syndrome

INTRODUCTION

Oculofaciocardiodental syndrome (OFCD, Mendelian Inheritance in Man (MIM) #300166), an X-linked dominant disorder, is characterized by ocular, facial, cardiac and dental abnormalities associated with male lethality.[1,2] Mutations in the BCL-6 corepressor gene (*BCOR*, MIM *300485) at Xp11.4 cause OFCD.[3] *BCOR/Bcor* is ubiquitously expressed in human tissues and is strongly and specifically expressed in the eye, brain, neural tube and branchial arches during mouse embryonic development, which are affected in OFCD.[4,5] In 2009, Hilton *et al.*[6] clinically reviewed 35 cases with *BCOR* mutations and summarized the frequency of phenotypes: congenital cataract (100%), microphthalmia and/or microcornea (82%), facial dysmorphism (96%) including long narrow face and high nasal bridge, cardiac anomalies (74%, commonly septal defects), dental abnormalities (100%) such as delayed and/or primary dentition, root radiculomegaly, and absent/duplicated/fused teeth and mental retardation (18%).[6] Additionally, skeletal abnormalities such as 2nd–3rd toe syndactyly, hammer toes, and radioulnar synostosis are also observed in 97% patients. Various types of mutations in *BCOR* have been described including nonsense, small insertions or deletions and splice site mutations, suggesting that the loss of functions (null allele) might result in OFCD. In addition, microdeletions involving *BCOR* have been also reported in individuals with OFCD. Most mutations predicted to generate premature stop codons, likely suffering from nonsense-mediated mRNA decay, although nonsense-mediated mRNA decay was unable to be confirmed because of the severe skewed X-inactivation in blood leukocytes.[3,6]

Nance–Horan syndrome (NHS) is an X-linked cataract-dental syndrome (MIM #302350) characterized by congenital cataract, dental abnormalities, facial dysmorphism and mental retardation.[7] Congenital cataract in affected male usually requires early surgery.[8] Dental abnormalities include maxillary and mandibular diastema of both central and lateral incisors, and screwdriver-shaped teeth because of narrow gingival and incisal margins.[9] Carrier females typically display posterior Y-sutural lens opacities, and the dental and facial anomalies of the syndrome may be observed, but with a milder presentation.[8] Mutations in *NHS* (MIM *300457) at Xp21.1-p22.3 cause NHS.[9–11] The most pathogenic mutations are truncating mutations. Coccia *et al.*[8] reported complex duplication-triplication rearrangements of the *NHS* gene in a family with congenital cataract and congenital

[1]Department of Human Genetics, Yokohama City University Graduate School of Medicine, Yokohama, Japan; [2]Department of Obstetrics and Gynecology, Asahikawa Medical College, Asahikawa, Japan and [3]Department of Ophthalmology, Seoul National University College of Medicine, Seoul, Korea
Correspondence: Dr N Matsumoto, Department of Human Genetics, Yokohama City University Graduate School of Medicine, Fukuura 3-9, Kanazawa-ku, Yokohama 236-0004, Japan.
E-mail: naomat@yokohama-cu.ac.jp
Received 3 October 2011; revised 6 December 2011; accepted 5 January 2012; published online 2 February 2012

heart defects in affected males, suggesting that genomic rearrangements of *NHS* are able to cause the X-linked cataract.

In this report, mutation screening and genomic microarray revealed a heterozygous mutation in *BCOR* and genomic rearrangements involving *NHS* in the three affected females of a Korean family with congenital cataract, dental abnormalities and 2nd–3rd toe syndactyly. Detailed molecular analysis will be presented.

MATERIALS AND METHODS

Clinical report

The Korean family with congenital cataract was previously described (as family 4) (Figure 1a).[12] Clinical features are summarized in Table 1. In the elder sister (MC17, the proband), bilateral congenital cataracts were noted 100 days after birth. Bilateral lensectomy and secondary intraocular lens insertion were performed. Ventricular septal defect, atrial septal defect, patent ductus arteriosus, delayed dentition, bilateral broad halluces, bilateral 2nd–3rd toe syndactyly, bilateral hammer toes and right brachyphalangia of fourth toe were also recognized. Mental development was normal. In the younger sister (MC18), bilateral congenital cataracts were also recognized. Bilateral lensectomy and secondary intraocular lens insertion were performed at ages of 2 months and 3 years, respectively. Right inguinal hernia, delayed dentition, and bilateral broad halluces, bilateral 2nd–3rd toe syndactyly, and bilateral hammer toes were noted (Figures 1b and c). She had learning difficulties at school, but IQ was not measured. In the mother (MC17b), bilateral congenital cataracts were noted and left lensectomy was performed at age of 10 years. Because of her dental anomalies and hypodontia, all her teeth were surgically removed. Bilateral 2nd–3rd toe syndactyly and bilateral hammer toes were noted. Her intelligence was normal. All the three affected members shared bilateral congenital cataracts, delayed dentition, bilateral 2nd–3rd toe syndactyly and bilateral hammer toes. Dysmorphic facial features were unseen.

DNA sequencing

Experimental protocols were approved by Institutional Review Boards for Ethical Issues at Yokohama City University School of Medicine and the Committee for the Ethical Issues on Human Genome and Gene Analysis, Seoul National University. Informed consent was obtained from all individuals. Genomic DNA was obtained from peripheral leukocytes using QIAGEN Blood and Cell Culture DNA Midi Kit (QIAGEN, Hilden, Germany). DNA was amplified using GenomiPhi V2 kit (GE healthcare, Buckinghamshire, UK). In *BCOR*, there are three isoforms: isoform a (GenBank accession number NM_017745.5), isoform b (GenBank accession number NM_001123384.1) and isoform c (GenBank accession number NM_001123385.1). In *NHS*, there are two isoforms: isoform 1 (GenBank accession number NM_198270.2) and isoform 2 (GenBank accession number NM_001136024.2). Nucleotide sequences of 1st to 15th exons of *BCOR* and 1st to 8th exons of *NHS* covering all the protein coding region as well as exon–intron borders were analyzed. Polymerase chain reaction (PCR) conditions and primer information are shown in Supplementary Table 1. PCR products were purified with ExoSAP (USB, Cleveland, OH, USA) and sequenced with BigDye terminator 3.1 (Applied Biosystems, Foster City, CA, USA) on 3100 and 3500×l Genetic Analyzer (Applied Biosystems). Sequences of patients were compared with the reference human genome sequences (based on the UCSC Genome Browser coordinate, February 2009) with Sequencher 4.10.1. (Gene Codes, Ann Arbor, MI, USA).

Copy number analysis

Copy number variations (CNVs) were investigated by Cytogenetics Whole-Genome 2.7 M. Array (Affymetrix, Santa Clara, CA, USA) based on the manufacturer's instruction using 100 ng genomic DNA from three affected females (MC17b, MC17 and MC18). Copy number alterations were analyzed by Chromosome Analysis Suite (Affymetrix) with NetAffx 30.1 annotations (hg18 assembly). Any filters such as minimum size and probe numbers of CNVs were not applied. The selection criteria for putative pathogenic CNVs were as follows: (1) CNVs were shared with three affected females, (2) CNVs encompassed exons and (3) CNVs were not present in the Database of Genomic Variants (http://projects.tcag.ca/variation/).

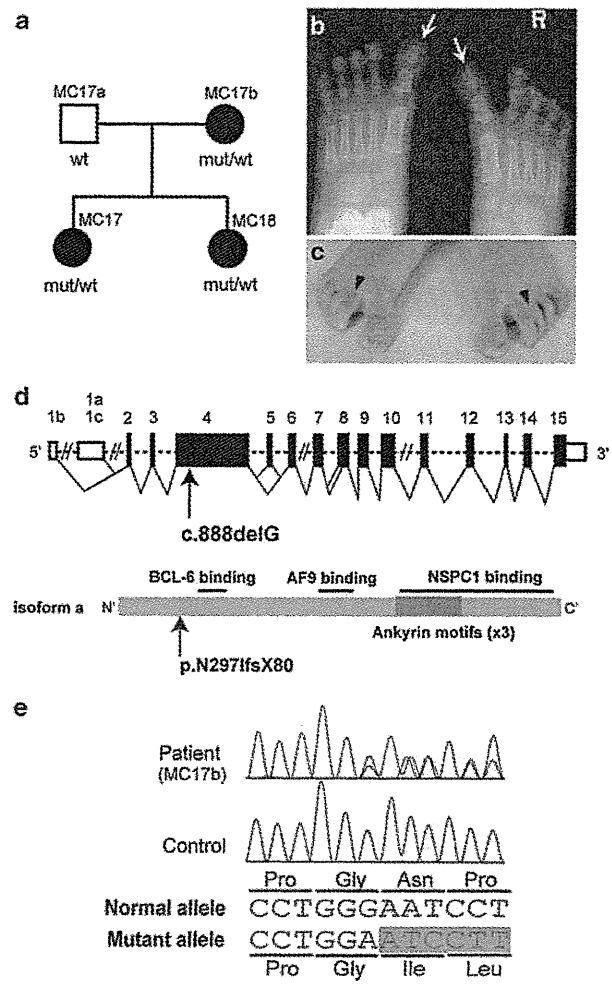

Figure 1 Pedigree, foot malformation and a *BCOR* mutation found in the family. **(a)** Familial pedigree. Black and open symbols denote affected and unaffected individuals, respectively. **(b, c)** Bilateral broad halluces (the big toe, arrows in **b**), bilateral 2nd–3rd cutaneous syndactyly (arrowheads in **c**) and bilateral hammer toes in MC18. **(d)** Schematic representation of the *BCOR* gene (top). UTR and coding region are open and filled rectangles, respectively. Alternative splicing by three different isoforms is shown. The isoform b is absence of exon 5 and the isoform c is 102bp and 156bp longer than the isoform a and b, respectively. The location of the c.888delG mutation is indicated by an arrow. The protein structure of BCOR (isoform a, bottom). Three consecutive ankyrin motifs are indicated as a dark-gray box. The three binding sites for BCL-6, AF9 and NSPC1 are indicated with horizontal bars. **(e)** Electropherograms showing the mutation in the affected patient (MC17b) (top) and a control (bottom). A single nucleotide deletion in exon 4 results in a frameshift. mut, a mutant allele; wt, a wild type allele.

Cloning of duplication breakpoints

DNA of the affected mother (MC17b) was digested with restriction enzymes: *Eco*RI, *Nsi*I, *Xba*I, *Bam*HI and *Bgl*II (New England Biolabs, Beverly, MA, USA). Digested DNA was self-ligated by Ligation High ver. 2 (Toyobo, Osaka, Japan), precipitated with ethanol, and dissolved in 20 µl EB buffer (QIAGEN, Tokyo, Japan). Inverse PCR was performed in 25 µl volume containing 2 µl ligated DNA, 1× PCR buffer for KOD FX, 0.4 mM each dNTPs, 0.5 µM each primer and

Table 1 Clinical features of patients with a *BCOR* mutation

	MC17b	*MC17*	*MC18*
Age	41	11	8
Sex	Female	Female	Female
Ocular features			
Congenital cataract	+	+	+
Microphthalmia/microcornea	–	–	–
Coloboma	–	–	–
Ptosis	–	–	–
Secondary glaucoma	–	+	+
Nystagmus	–	–	–
Cardiac features	–	+	–
Septal defects	–	+	–
Patent ductus arteriosus	–	+	–
Dental features			
Delayed/persistent/unerupted dentition	+	+	+
Root radiculomegaly (secondary teeth)	ND	ND	ND
Hypodontia (secondary teeth)	+	ND	ND
Duplication/fusion (secondary teeth)	ND	ND	ND
Skeletal features			
Hammer toes (camptodactyly)	+	+	+
Second–third toe syndactyly	+	+	+
Broad halluces (big toe)	–	+	+
Brachyphalangia of the fourth right toe	–	+	–
Radioulnar synostosis	ND	ND	ND
Lodosis/scoliosis/vertebral fusion	ND	ND	ND
Other features			
Mental retardation	–	–	+
Hearing impairment	–	ND	ND
Inguinal hernia	–	–	+

Abbreviation: ND, Not determined.
A plus (+) or minus (–) sign denotes the presence or absence of a particular physical feature.

0.5 U KOD FX polymerase (Toyobo). PCR were cycled 35 times at 98 °C for 10 s, 68 °C for 10 min. PCR products electrophoresed in 1% agarose gel were stained with ethidium bromide and the aberrant band was extracted using QIAEXII Gel Extraction Kit (QIAGEN, Tokyo, Japan) and sequenced. Primer information is available on request.

X inactivation study and haplotype analysis

X inactivation pattern was studied using the human androgen receptor assay and fragile X mental retardation locus methylation assay as previously described.[13–15] Briefly, genomic DNA of a patient (MC17), the parents (MC17a and MC17b), a control male and a control female was digested with two methylation-sensitive enzymes, *Hpa*II and *Hha*I. PCR was performed with human androgen receptor assay primers (FAM-labeled ARf: 5′-CCAGAAT CTGTTCCAGAGCGTGC-3′; ARr: 5′-CTCTACGATGGGCTTGGGGAGAA C-3′)[16] and fragile X mental retardation assay primers (FAM-labeled FMR1f: 5′-AGCCCCGCACTTCCACCACCAGCTCCTCCA-3′; FMR1r: 5′-GCTCAGCT CCGTTTCGGTTTCACTTCCGGT-3′). Fluorescent-labeled products were analyzed on an ABI PRISM 3100 or 3130×l Genetic analyzer and GeneMapper Software version 4.0 (Applied Biosystems). One of affected females (MC18) was not analyzed because of insufficient amount of genomic DNA. According to published criteria, X inactivation ratios of ⩽80:20 were considered random and ratios >80:20 were considered skewed and ratios >90:10 were considered highly skewed.[16,17]

X chromosome haplotype was analyzed using 12 microsatellite markers (*DXS1060, DXS8051, DXS987, DXS1226, DXS1214, DXS1068, DXS993, DXS991, DXS986, DXS8055, DXS1047* and *DXS1073*). Fluorescent- labeled (either FAM, VIC or NED) forward primers and tailed reverse primers were purchased from Applied Biosystems. These markers were based on the Marshfield genetic map (http://research.marshfieldclinic.org/genetics). PCR was cycled 40 times at 94 °C for 30 s, 55 °C for 30 s and 72 °C for 30 s in 10 μl volume containing 50 ng DNA, 1× ExTaq buffer, 0.2 mM each dNTP, 0.4 μM each primer and 0.1 U ExTaq HS polymerase. Haplotypes were manually constructed.

RESULTS

We detected a *BCOR* mutation, c. 888delG in MC17, MC17b and MC18 (Figures 1d and e). The mutation may result in insertion of 80 new amino acids after the mutation site with a premature stop codon at position 377 (p.N297IfsX80). The mutation was completely co-segregated with OFCD phenotypes in this family (Figure 1a). Sequencing of the entire *NHS* coding region detected no pathological mutations in this family.

The Cytogenetics Whole-Genome 2.7 M array detected a total of 48 CNVs (12 duplications and 36 deletions) in any of the affected females. The CNVs, which encompassed exons, were 8 duplications and 13 deletions. Among them, two duplications and one deletion were shared with three affected females. The one deletion was present in the Database of Genomic Variants. Thus, the CNVs fulfilling the criteria for pathogenic CNVs were two interstitial duplications. The 740-kb duplication at Xp22.2–22.13 encompassed exons 2–18 of *REPS2* (MIM *300317) and exons 1–3 of *NHS*. The other 110-kb duplication at Xp21.3 contained exon 2 of interleukin-1 receptor accessory protein-like 1 (*IL1RAPL1*) (MIM *300206) (Figure 2a). We were unable to examine the duplications by fluorescent *in situ* hybridization because only DNA samples were available. Instead, inverse PCR of self-ligated DNA with different sets of primers was able to amplify an expected fragment from normal *NHS* allele in all sets of primers, suggesting that the presence of one or more normal *NHS* alleles (Figures 2b and c). In addition, several attempts successfully cloned one of rearrangement junctions in relation to *NHS* (Figure 2c). This aberrant band showed that the sequences of intron 1 of *IL1RAPL1* followed the sequences of intron 3 of *NHS*, suggesting that two duplications were tandemly connected (Figure 2d, upper cases). More complicatedly, 62-bp sequences of intron 3 of *IL1RAPL1* with inverted orientation were inserted between intron 3 of *NHS* and intron 1 of *IL1RAPL1* (Figure 2d, lower cases). The other possible breakpoints, which may result in disruption of *NHS* locus could not be determined regardless of rigorous attempts. Thus there seems to be two normal *NHS* alleles and an extra *NHS* allele, in which exons 1–3 of *NHS* was connected to exon 2 of *IL1RAPL1*. Copy number of the *BCOR* gene was normal. In human androgen receptor assays, the mother (MC17b) was skewed pattern (8%), whereas the elder sister (MC17) showed a random pattern (26%). In fragile X mental retardation assays, the mother (MC17b) and elder sister (MC17) showed a highly skewed pattern (<1%) and a random pattern (48%), respectively. X-chromosome haplotype analysis was able to separate all the alleles in this family (Supplementary Figure 1). The inactivated allele in the mother harbored the *BCOR* mutation and the *NHS* rearrangement.

DISCUSSION

BCOR functions as a corepressor of BCL-6, which is a POZ/zinc finger transcription repressor.[4] BCOR have three consecutive ankyrin motifs, an AF9 (ALL1 fused gene from chromosome 9) binding site and an NSPC1 (nervous system polycomb-1) binding site.[4,18,19] Recently, the

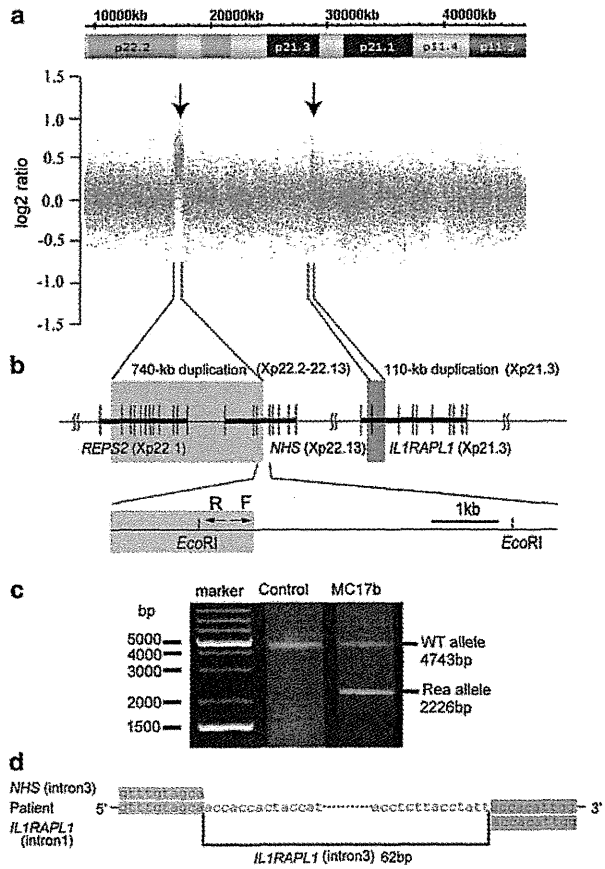

Figure 2 Two microduplications at Xp22.2–22.13 and Xp21.3. (**a**) Array profile of a part of chromosome X in the elder sister (MC17). *x* and *y* axis show the genomic location from the p telomere of chromosome X (UCSC coordinates, May, 2006) (upper) and $\log_2$ (Signal ratio) values (lower), respectively. The 740-kb duplication at Xp22.2–22.13 and the 110-kb duplication at Xp21.3 are indicated by arrows. (**b**) Upper shows schematic representation of two duplicated regions (highlighted in gray). Three genes (*REPS2*, *NHS* and *IL1RAPL1*) are oriented in the same direction (from centromere to telomere). Lower indicates scheme of inverse PCR using self-ligated DNA after digestion with *Eco*RI. Primers are shown by arrows (F, forward; R, reverse). (**c**) Gel image of inverse PCR products performed as shown in (**b**). Upper and lower bands represent wild-type allele (WT allele) and rearranged allele (Rea allele), respectively. The DNA of both bands was extracted from agarose gel and sequenced. (**d**) Sequence of a Rea allele is shown. The top, middle and bottom indicate sequences of the intron 3 of *NHS*, rearranged junction and intron 1 of *IL1RAPL1*, respectively. The 62 nucleotides of intron 3 of *IL1RAPL1* (lower cases) were inserted in an inverted orientation between intron 3 of *NHS* and intron 1 of *IL1RAPL1*. Matched sequences are highlighted with gray shadows.

minimal BCL-6 binding site was identified within residues 498–514, which is located in exon 4.[20] In this study, a novel *BCOR* mutation, c.888delG (p.N297IfsX80) in exon 4, was found in this family. We assumed the mutant transcript with this mutation may undergo nonsense-mediated mRNA decay, but we could not confirm it as no living cells were available from the patients. A total of 31 mutations in *BCOR* were registered in Human Gene Mutation Database (http://www.biobase-international.com/). All the mutations result in premature stop codons. Exon 4 harbors 40% of mutations (12/30), leading to truncated proteins lacking BCL-6, AF9 and NSPC1 binding sites, and ankyrin motifs if translated. Lack of BCL-6 binding site could not explain the OFCD phenotypes because BCL-6-deficient mice did not show ocular, dental and skeletal phenotypes.[21,22] Moreover, an OFCD mutant protein, that lacked ankyrin motifs and NSPC1 binding site, showed transcriptional repression activity similar to that of wild type.[3] Thus, the c.888delG mutation in *BCOR* may be associated with loss of *BCOR* transcripts through nonsense-mediated mRNA decay.

By genomic microarray, two microduplications were detected in MC17, MC18 and MC17b: one at Xp22.2–22.13 involving a part of *REPS2* and *NHS*, and the other at Xp21.3 containing exon 2 of *IL1RAPL1*. Previously, complex duplication-triplication rearrangements of the *NHS* gene in a family with congenital cataract were reported, suggesting that genomic rearrangements of *NHS* are able to cause the X-linked cataract.[8] This family did not show the typical features of NHS such as dental anomalies, dysmorphism and developmental delay, and congenital heart defects were diagnosed in four out of six affected males. The complex rearrangement consists of triplication embedded within a duplication region. The triplicated region includes the *NHS* genes except exon 1, and the entire *SCML1* and *RAI2* genes. Coccia *et al.*[8] described that the additional phenotype of congenital heart defects observed in some affected males could be because of perturbed *NHS* gene transcription or increased dosage of the *NHS*, *SCML1* or *RAI2* genes. In our cases, two normal *NHS* alleles may exist in addition to an extra *NHS* allele, in which exons 1–3 of *NHS* was connected to individual exon 2 of *IL1RAPL1*, keeping the protein coding frame if properly spliced. Because the transcript from the extra *NHS* allele did not have polyA signal sequences, the allele is likely to produce no functional protein. Thus, the situation was totally different between our cases and Coccia's *et al.*'s[8] cases.

Recently, Honda *et al.*[23] reported two unrelated X-linked mental retardation Japanese families, which possessed the similar duplication found in our Korean family: the 737-kb duplication at Xp22.2, which contains a part of *REPS2* and *NHS*, and the 100-kb duplication at Xp21.3, which contains a part of *IL1RAPL1*. In their report, fluorescent *in situ* hybridization analysis revealed that the clone RP11-438J7, which entirely covered the duplication at Xp21.3, demonstrated two distinct signals at Xp in metaphases, suggesting that the duplication at Xp21.3 was inserted separately from the original site. The clone RP11-2K15 at Xp22.2, spanning the breakpoint of *REPS2*, showed one bright strong signal, suggesting that the duplication at Xp22.2 occurred in the proximity. Interestingly, the one of two signals of the RP11-438J7 was close to that of RP11-2K15 at Xp22.2, suggesting that the duplication involving *IL1RAPL1* was inserted at Xp22.2. Their result is consistent with our data of the duplication breakpoint, in which the breakpoint in *NHS* was connected with the breakpoint of *IL1RAPL1*. Based on our experiences, high-density array experiments of >500 Japanese cases never showed such the genomic rearrangement involving *NHS*, implying that the rearrangement is very rare in Japanese population. It is noteworthy that congenital cataract and dental abnormalities were not pointed out in all the members (males and carrier females).[23] Thus, it is unlikely that the genomic rearrangement involving *NHS* causes congenital cataract and dental abnormalities as found in our family.

IL1RAPL1 is a causative gene for X-linked mental retardation,[24] and the microduplication at Xp21.3 containing exon 2 of *IL1RAPL1* was suggested to cause MR in affected males.[23] Most carrier females of *IL1RAPL1* mutations and the carrier mother of the microduplication involving *IL1RAPL1* showed normal intelligence.[23–25] In this study, one of the three affected females (MC18) had learning difficulties at school, which could be mild presentation of MR. As 18% of patients with *BCOR* mutations showed MR,[6] it is reasonable that the *BCOR* mutation, rather than *IL1RAPL1* rearrangement, causes mild MR in MC18.

Skewed and random X-inactivation in the mother (MC17b) and the elder daughter (MC17) was confirmed, respectively, in this family. In OFCD, skewed X-inactivation with the preferential inactivation of the mutated allele were recognized in eight affected females (like the mother, MC17b), suggesting that the *BCOR* mutations may lead to a selective disadvantage in blood leukocytes.[3,26] However, it has been reported that the X-inactivation pattern in blood leukocytes are unable to determine the severity of disease phenotypes as X-inactivation pattern may vary among tissues.[27] We suspect that X-inactivation pattern is different between peripheral blood leukocytes and respective tissues associated with OFCD phenotype.

In conclusion, a new OFCD family is described with a novel *BCOR* mutation. Clinical features overlap between OFCD and NHS, both of which belong to a spectrum of X-linked microphthalmia disorders.[6] Our cases have a *BCOR* mutation and genomic rearrangements involving *NHS*, confusing us to address the genetic etiology in the family. However, the presence of bilateral 2nd–3rd toe syndactyly and septal heart defects, which is unique to OFCD, can lead us to the conclusion that the *BCOR* mutation is the major determinant for the phenotypes in this family. Careful examination of associated anomalies will be useful for genetic testing of X-linked microphthalmia disorders.

ACKNOWLEDGEMENTS

We thank the family members for their participation in this study. This work was supported by Research Grants from the Ministry of Health, Labour and Welfare (HS, N Miyake and N Matsumoto) and the Japan Science and Technology Agency (N Matsumoto) and Grant-in-Aid for Scientific Research from Japan Society for the Promotion of Science (N Matsumoto).

Web Resources

The URLs for data presented herein are as follows: UCSC Genome Browser, http://genome.ucsc.edu/cgi-bin/hgGateway

1 Wilkie, A. O., Taylor, D., Scambler, P. J. & Baraitser, M. Congenital cataract, microphthalmia and septal heart defect in two generations: a new syndrome? *Clin. Dysmorphol.* **2,** 114–119 (1993).
2 Aalfs, C. M., Oosterwijk, J. C., van Schooneveld, M. J., Begeman, C. J., Wabeke, K. B. & Hennekam, R. C. Cataracts, radiculomegaly, septal heart defects and hearing loss in two unrelated adult females with normal intelligence and similar facial appearance: confirmation of a syndrome? *Clin. Dysmorphol.* **5,** 93–103 (1996).
3 Ng, D., Thakker, N., Corcoran, C. M., Donnai, D., Perveen, R., Schneider, A. *et al.* Oculofaciocardiodental and Lenz microphthalmia syndromes result from distinct classes of mutations in *BCOR*. *Nat. Genet.* **36,** 411–416 (2004).
4 Huynh, K. D., Fischle, W., Verdin, E. & Bardwell, V. J. BCoR, a novel corepressor involved in BCL-6 repression. *Genes Dev.* **14,** 1810–1823 (2000).
5 Wamstad, J. A. & Bardwell, V. J. Characterization of *Bcor* expression in mouse development. *Gene Expr. Patterns* **7,** 550–557 (2007).
6 Hilton, E., Johnston, J., Whalen, S., Okamoto, N., Hatsukawa, Y., Nishio, J. *et al. BCOR* analysis in patients with OFCD and Lenz microphthalmia syndromes, mental retardation with ocular anomalies, and cardiac laterality defects. *Eur. J. Hum. Genet.* **17,** 1325–1335 (2009).
7 Nance, W. E., Warburg, M., Bixler, D. & Helveston, E. M. Congenital X-linked cataract, dental anomalies and brachymetacarpalia. *Birth Defects Orig. Artic. Ser.* **10,** 285–291 (1974).
8 Coccia, M., Brooks, S. P., Webb, T. R., Christodoulou, K., Wozniak, I. O., Murday, V. *et al.* X-linked cataract and Nance-Horan syndrome are allelic disorders. *Hum. Mol. Genet.* **18,** 2643–2655 (2009).
9 Lewis, R. A., Nussbaum, R. L. & Stambolian, D. Mapping X-linked ophthalmic diseases. IV. Provisional assignment of the locus for X-linked congenital cataracts and microcornea (the Nance-Horan syndrome) to Xp22.2-p22.3. *Ophthalmology.* **97,** 110–120; discussion 120–111 (1990).
10 Stambolian, D., Lewis, R. A., Buetow, K., Bond, A. & Nussbaum, R. Nance-Horan syndrome: localization within the region Xp21.1-Xp22.3 by linkage analysis. *Am. J. Hum. Genet.* **47,** 13–19 (1990).
11 Burdon, K. P., McKay, J. D., Sale, M. M., Russell-Eggitt, I. M., Mackey, D. A., Wirth, M. G. *et al.* Mutations in a novel gene, *NHS*, cause the pleiotropic effects of Nance-Horan syndrome, including severe congenital cataract, dental anomalies, and mental retardation. *Am. J. Hum. Genet.* **73,** 1120–1130 (2003).
12 Miyamoto, T., Yu, Y. S., Sato, H., Hayashi, H., Sakugawa, N., Ishikawa, M. *et al.* Mutational analysis of the human *MBX* gene in four Korean families demonstrating microphthalmia with congenital cataract. *Turk J. Pediatr.* **49,** 334–336 (2007).
13 Allen, R. C., Zoghbi, H. Y., Moseley, A. B., Rosenblatt, H. M. & Belmont, J. W. Methylation of *Hpa*II and *Hha*I sites near the polymorphic CAG repeat in the human androgen-receptor gene correlates with X chromosome inactivation. *Am. J. Hum. Genet.* **51,** 1229–1239 (1992).
14 Carrel, L. & Willard, H. F. An assay for X inactivation based on differential methylation at the fragile X locus, *FMR1*. *Am. J. Med. Genet.* **64,** 27–30 (1996).
15 Nishimura-Tadaki, A., Wada, T., Bano, G., Gough, K., Warner, J., Kosho, T. *et al.* Breakpoint determination of X; autosome balanced translocations in four patients with premature ovarian failure. *J. Hum. Genet.* **56,** 156–160 (2011).
16 Kubota, T., Nonoyama, S., Tonoki, H., Masuno, M., Imaizumi, K., Kojima, M. *et al.* A new assay for the analysis of X-chromosome inactivation based on methylation-specific PCR. *Hum. Genet.* **104,** 49–55 (1999).
17 Amos-Landgraf, J. M., Cottle, A., Plenge, R. M., Friez, M., Schwartz, C. E., Longshore, J. *et al.* X chromosome-inactivation patterns of 1,005 phenotypically unaffected females. *Am. J. Hum. Genet.* **79,** 493–499 (2006).
18 Srinivasan, R. S., de Erkenez, A. C. & Hemenway, C. S. The mixed lineage leukemia fusion partner AF9 binds specific isoforms of the BCL-6 corepressor. *Oncogene* **22,** 3395–3406 (2003).
19 Gearhart, M. D., Corcoran, C. M., Wamstad, J. A. & Bardwell, V. J. Polycomb group and SCF ubiquitin ligases are found in a novel BCOR complex that is recruited to BCL6 targets. *Mol. Cell Biol.* **26,** 6880–6889 (2006).
20 Ghetu, A. F., Corcoran, C. M., Cerchietti, L., Bardwell, V. J., Melnick, A. & Prive, G. G. Structure of a BCOR corepressor peptide in complex with the BCL6 BTB domain dimer. *Mol. Cell.* **29,** 384–391 (2008).
21 Ye, B. H., Cattoretti, G., Shen, Q., Zhang, J., Hawe, N., de Waard, R. *et al.* The *BCL-6* proto-oncogene controls germinal-centre formation and Th2-type inflammation. *Nat. Genet.* **16,** 161–170 (1997).
22 Dent, A. L., Shaffer, A. L., Yu, X., Allman, D. & Staudt, L. M. Control of inflammation, cytokine expression, and germinal center formation by BCL-6. *Science* **276,** 589–592 (1997).
23 Honda, S., Hayashi, S., Imoto, I., Toyama, J., Okazawa, H., Nakagawa, E. *et al.* Copy-number variations on the X chromosome in Japanese patients with mental retardation detected by array-based comparative genomic hybridization analysis. *J. Hum. Genet.* **55,** 590–599 (2010).
24 Carrie, A., Jun, L., Bienvenu, T., Vinet, M. C., McDonell, N., Couvert, P. *et al.* A new member of the IL-1 receptor family highly expressed in hippocampus and involved in X-linked mental retardation. *Nat. Genet.* **23,** 25–31 (1999).
25 Nawara, M., Klapecki, J., Borg, K., Jurek, M., Moreno, S., Tryfon, J. *et al.* Novel mutation of *IL1RAPL1* gene in a nonspecific X-linked mental retardation (MRX) family. *Am. J. Med. Genet. A* **146A,** 3167–3172 (2008).
26 Hedera, P. & Gorski, J. L. Oculo-facio-cardio-dental syndrome: skewed X chromosome inactivation in mother and daughter suggest X-linked dominant Inheritance. *Am. J. Med. Genet. A* **123A,** 261–266 (2003).
27 Bartnik, M., Derwinska, K., Gos, M., Obersztyn, E., Kolodziejska, K. E., Erez, A. *et al.* Early-onset seizures due to mosaic exonic deletions of *CDKL5* in a male and two females. *Genet. Med.* **13,** 447–452 (2011).

Supplementary Information accompanies the paper on Journal of Human Genetics website (http://www.nature.com/jhg)

ELSEVIER

Brain & Development 34 (2012) 364–367

BRAIN & DEVELOPMENT
Official Journal of the Japanese Society of Child Neurology

www.elsevier.com/locate/braindev

Case report

A girl with early-onset epileptic encephalopathy associated with microdeletion involving *CDKL5*

Hirotomo Saitsu [a,*], Hitoshi Osaka [b], Kiyomi Nishiyama [a], Yoshinori Tsurusaki [a], Hiroshi Doi [a], Noriko Miyake [a], Naomichi Matsumoto [a]

[a] *Department of Human Genetics, Yokohama City University Graduate School of Medicine, Yokohama, Japan*
[b] *Division of Neurology, Clinical Research Institute, Kanagawa Children's Medical Center, Yokohama, Japan*

Received 28 March 2011; received in revised form 21 June 2011; accepted 5 July 2011

Abstract

Recent studies have shown that aberrations of *CDKL5* in female patients cause early-onset intractable seizures, severe developmental delay or regression, and Rett syndrome-like features. We report on a Japanese girl with early-onset epileptic encephalopathy, hypotonia, developmental regression, and Rett syndrome-like features. The patient showed generalized tonic seizures, and later, massive myoclonus induced by phone and light stimuli. Brain magnetic resonance imaging showed no structural brain anomalies but cerebral atrophy. Electroencephalogram showed frontal dominant diffuse poly spikes and waves. Through copy number analysis by genomic microarray, we found a microdeletion at Xp22.13. A *de novo* 137-kb deletion, involving exons 5–21 of *CDKL5*, *RSI*, and part of *PPEF1* gene, was confirmed by quantitative PCR and breakpoint specific PCR analyses. Our report suggests that the clinical features associated with *CDKL5* deletions could be implicated in Japanese patients, and that genetic testing of *CDKL5*, including both sequencing and deletion analyses, should be considered in girls with early-onset epileptic encephalopathy and RTT-like features.
© 2011 The Japanese Society of Child Neurology. Published by Elsevier B.V. All rights reserved.

Keywords: *CDKL5*; Microdeletion; Early-onset epileptic encephalopathy; Rett syndrome-like features

1. Introduction

Mutations in the *CDKL5* (cyclin-dependent kinase-like 5) gene are associated with early-onset intractable seizures, infantile spasms, severe developmental delay, and Rett syndrome (RTT)-like features [1–4]. High-resolution genomic microarray enables us to detect copy number variations (CNVs) involving *CDKL5* gene in girls with severe epileptic encephalopathy and a RTT-like phenotype, suggesting that *CDKL5*-related CNVs can cause epileptic encephalopathy [4–8]. However, Japanese phenotypes associated with *CDKL5* deletions have never been described. Detailed clinical and molecular data of the patient will be presented.

2. Case report

A 12-year old girl is a product of unrelated healthy parents (both Japanese). She was born at term without asphyxia after an uneventful pregnancy. Her birth weight was 3240 g and head circumference was 31.0 cm (−1.2 SD). She gained head control at 4 months and could sit without support at 8 months. She exhibited generalized tonic seizures with both eyes' deviation at 6 months of age. These seizures were often precipitated when light was turned on. Treatment with valproic acid

* Corresponding author. Address: Department of Human Genetics, Yokohama City University Graduate School of Medicine, 3-9 Fukuura, Kanazawa-ku, Yokohama 236-0004, Japan. Tel.: +81 45 787 2606; fax: +81 45 786 5219.
E-mail address: hsaitsu@yokohama-cu.ac.jp (H. Saitsu).

0387-7604/$ - see front matter © 2011 The Japanese Society of Child Neurology. Published by Elsevier B.V. All rights reserved.
doi:10.1016/j.braindev.2011.07.004

was initiated and only partially effective. She was referred to Kanagawa Children's Medical Center at age 15 months for an evaluation and control of seizures. She showed poor eye fixation and pursuit. Her muscle tone was hypotonic. Deep tendon reflexes were within normal range and bilateral extensor plantar responses were not observed. Her head circumference was 46.2 cm (+0.3 SD). Electroencephalogram (EEG) showed frontal dominant diffuse polyspikes and waves (Fig. 1A). Clonazepam was initiated for daily tonic seizures with eye blinking. Massive myoclonus as well as tonic seizures induced by phone and light stimuli was observed at 22 months. EEG revealed the polyspike-and-slow wave complex with myoclonus (Fig. 1B). However, EEG failed to show the photo/phone sensitivity and zonisamide was added. Although there were no clear fever-sensitive seizures, she was diagnosed as borderline severe myoclonic epilepsy in infancy. She could walk without assistance at 2 years. Brain magnetic resonance imaging showed the completion of myelination with mild cerebral atrophy (Fig. 1D–F). Although multifocal spikes are consistently observed at EEG (Fig. 1C), seizure frequency decreased around 10 years old without change of medications. Her development is severely delayed and her developmental quotient, 32 at 2 years and 9 months, decreased to 19 at 7 years. She cannot speak any words now and goes to special educational school with no seizures. She shows some Rett-like features, such as hand apraxia, bruxism, and sleep disturbances, but no hand stereotypes, acquired microcephaly or loss of purposeful hand skills.

STXBP1 [9] was not mutated by high resolution melting analysis. To screen copy number alterations associated with seizures, we performed whole-genome 2.7 M Array analysis (Affymetrix, Santa Clara, CA). A 137-kb microdeletion at Xp22.13, which contained a total of three RefSeq genes including exons 5–21 of *CDKL5* (transcript variant 1, Genebank accession number NM_003159.2), was found (Fig. 2A). No other pathogenic CNVs were observed. Quantitative PCR targeted for exons 2, 5, and 21 of *CDKL5*, and breakpoint specific PCR analysis of the family showed that the deletion occurred *de novo* (Fig. 2B and C). Sequence of the junctional fragment confirmed a 137,593-bp deletion

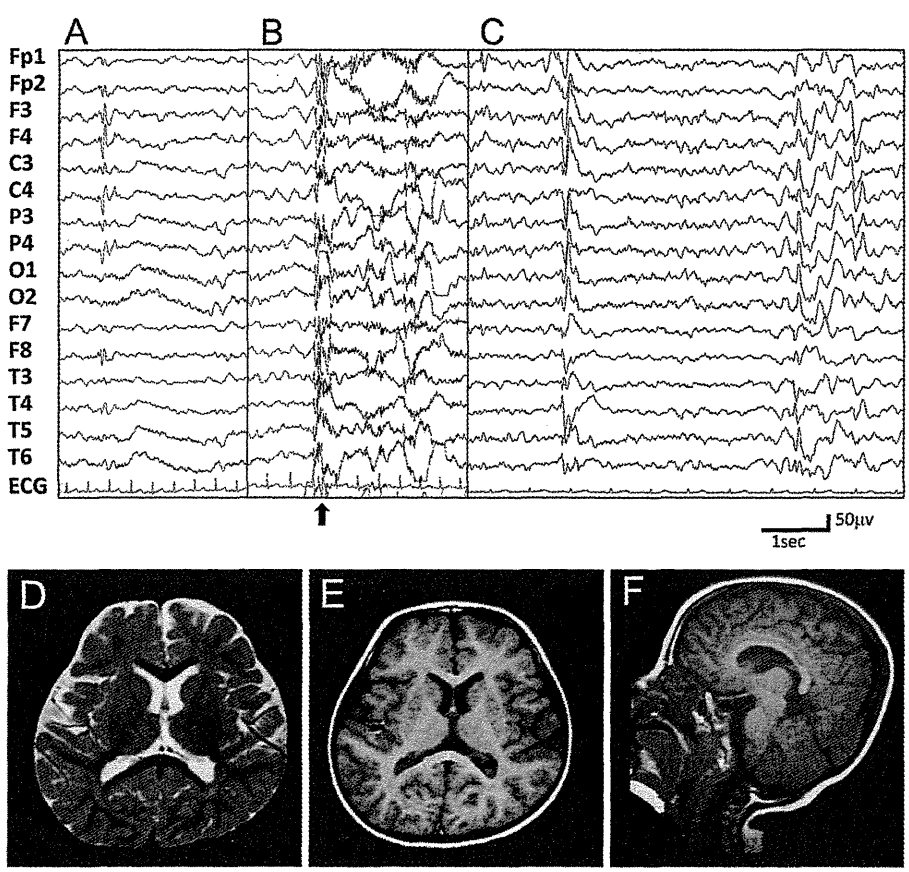

Fig. 1. Serial EEGs at 15 months (A), 22 months (B), and 9 years (C). EEG at 15 months showed occasional frontal dominant polyspikes-and-slow waves (A). EEG at 22 months showed the polyspike-and-slow wave complex and correlate with myoclonus (arrow in B). Independent multifocal spikes-and-slow waves were observed at EEG recorded at 9 years (C). Brain MRI at 2 years of age showed completion of myelination and mild cerebral atrophy in both T2 (D) and T1 (E) images. (F) Sagital image disclosed no cerebellar atrophy.

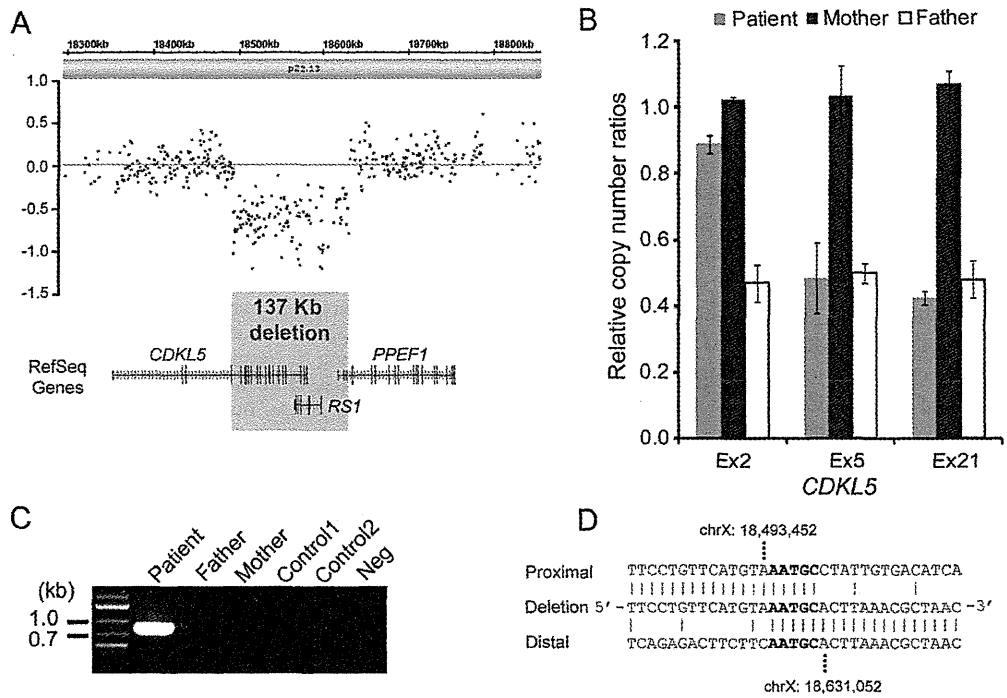

Fig. 2. A 137-kb deletion involving *CDKL5*. (A) 2.7 M array profile clearly showed a 137-kb deletion at Xp22.13 in the patient. A total of three RefSeq genes, including *CDKL5*, *RS1*, and *PPEF1*, were involved with the deletion (bottom). (B) Quantitative real-time PCR analysis of the patient and her parents. In the patient, while relative copy number ratios of non-deleted exon 2 showed 0.890 (near 1.0), that of deleted exon 5 and exon 21 showed 0.485 and 0.425 (both below 0.5), respectively, indicating a heterozygous deletion. Her parents did not show any abnormalities, suggesting that the deletion occurred *de novo*. (C) Breakpoint specific PCR analysis of the family of the patient. Primers flanking the deletion could successfully amplify a 851-bp product only from the patient, indicating the deletion occurred *de novo*. Neg, negative control (no template DNA). (D) Deletion junction sequence. Top, middle and bottom strands show proximal, deleted, and distal sequences, respectively. Overlapping five nucleotides were highlighted in bold.

(chrX: 18,493,457–18,631,052 bp). The presence of 5-bp microhomology at the deletion junction suggested nonhomologous end joining in the process of rearrangement (Fig. 2D). Human androgen receptor assay showed that X-inactivation was random (78:22) in the patient (data not shown). Primer sequences are available on request.

3. Discussion

To date, more than 50 mutations have been reported in females with early-onset epileptic encephalopathy and a RTT-like phenotype. Of note, the frequency of *CDKL5* mutations has been estimated to be about 8% in girls with early-onset seizures [4,5], suggesting that genetic testing of *CDKL5* mutations should be considered in girls with early-onset epileptic encephalopathy. Moreover, genomic deletions involving *CDKL5* gene have been reported in recent 3 years, and it has been shown that there is no obvious phenotypic difference between the patients with microdeletions and mutations [4–8].

Here we described a Japanese girl with a *de novo* microdeletion involving *CDKL5* gene. Because the microdeletion involved most exons of *CDKL5* (except exons 1–4), it is likely that the deletion is null allele for *CDKL5* function. Importantly, the patient showed common clinical features associated with *CDKL5* aberrations: an initial normal development followed by intractable early-onset seizures with developmental regression, hypotonia, poor eye fixation and pursuit, and Rett-like features including hand apraxia, bruxism, and absence of speech. Cerebral atrophy in brain MRI is also a common feature of *CDKL5* mutations. Although hand stereotypes and acquired microcephaly were negative in our patient, which were observed in 85% and 61.1% of patients with *CDKL5* mutations, respectively [3,4], our report suggests that the clinical features associated with *CDKL5* aberrations could be applicable in Japanese patients.

The seizure type in this patient seems to be atypical compared with the previous reports. Although various types of seizures including focal clonic, tonic, and myoclonic seizures were reported, infantile spasm has been observed ~80% patients with *CDKL5* aberrations [3,4]. The patient initially showed generalized tonic seizures with both eyes' deviation, then daily tonic seizures with eye blinking, but no infantile spasms. Of note, massive

myoclonus as well as tonic seizures was induced by phone and light stimuli, which were never reported in patients with *CDKL5* abnormalities. Thus, our report further highlighted that *CDKL5* abnormalities can cause a wide variety of seizures in affected children.

The microdeletion at Xp22.13 involved two other genes. *RS1* encodes an extracellular protein that plays a crucial role in the cellular organization of the retina. Mutations in *RS1* cause X-linked juvenile retinoschisis in only males (MIM +312,700). *PPEF1* encodes a member of the serine/threonine protein phosphatase with EF-hand motif family. Although *PPEF1* is related to *Drosophila* retinal degeneration C gene, deficiency of *Ppef1* did not cause retinal degeneration or seizures in mice [10]. Thus *RS1* and *PPEF1* are less likely to be involved in infantile epileptic encephalopathy. And no eye phenotypes were recognized in our patient.

In conclusion, we firstly described a Japanese girl with a genomic deletion involving *CDKL5* gene. Our report supports the importance of genetic testing of *CDKL5*, including both mutation and CNVs analysis, in girls with early-onset epileptic encephalopathy and RTT-like features.

Acknowledgements

We would like to thank the patient and her family for their participation in this study. This work was supported by Research Grants from the Ministry of Health, Labour and Welfare (H.S., H.O., N. Miyake and N. Matsumoto), Grant-in-Aid for Scientific Research from Japan Society for the Promotion of Science (N. Matsumoto), Grant-in-Aid for Young Scientist from Japan Society for the Promotion of Science (H.S.), Research Promotion Fund from Yokohama Foundation for Advancement of Medical Science (H.S. and H.O.), Research Grants from the Japan Epilepsy Research Foundation (H.S.), and Research Grant from Naito Foundation (N. Matsumoto).

References

[1] Kalscheuer VM, Tao J, Donnelly A, Hollway G, Schwinger E, Kubart S, et al. Disruption of the serine/threonine kinase 9 gene causes severe X-linked infantile spasms and mental retardation. Am J Hum Genet 2003;72:1401–11.

[2] Weaving LS, Christodoulou J, Williamson SL, Friend KL, McKenzie OL, Archer H, et al. Mutations of CDKL5 cause a severe neurodevelopmental disorder with infantile spasms and mental retardation. Am J Hum Genet 2004;75:1079–93.

[3] Bahi-Buisson N, Nectoux J, Rosas-Vargas H, Milh M, Boddaert N, Girard B, et al. Key clinical features to identify girls with CDKL5 mutations. Brain 2008;131(Pt 10):2647–61.

[4] Nemos C, Lambert L, Giuliano F, Doray B, Roubertie A, Goldenberg A, et al. Mutational spectrum of CDKL5 in early-onset encephalopathies: a study of a large collection of French patients and review of the literature. Clin Genet 2009;76:357–71.

[5] Mei D, Marini C, Novara F, Bernardina BD, Granata T, Fontana E, et al. Xp22.3 genomic deletions involving the CDKL5 gene in girls with early onset epileptic encephalopathy.. Epilepsia 2010;51:647–54.

[6] Bahi-Buisson N, Girard B, Gautier A, Nectoux J, Fichou Y, Saillour Y, et al. Epileptic encephalopathy in a girl with an interstitial deletion of Xp22 comprising promoter and exon 1 of the CDKL5 gene. Am J Med Genet B Neuropsychiatr Genet 2010;153B:202–7.

[7] Erez A, Patel AJ, Wang X, Xia Z, Bhatt SS, Craigen W, et al. Alu-specific microhomology-mediated deletions in CDKL5 in females with early-onset seizure disorder. Neurogenetics 2009;10:363–9.

[8] Russo S, Marchi M, Cogliati F, Bonati MT, Pintaudi M, Veneselli E, et al. Novel mutations in the CDKL5 gene, predicted effects and associated phenotypes. Neurogenetics 2009;10:241–50.

[9] Saitsu H, Kato M, Mizuguchi T, Hamada K, Osaka H, Tohyama J, et al. De novo mutations in the gene encoding STXBP1 (MUNC18-1) cause early infantile epileptic encephalopathy. Nat Genet 2008;40:782–8.

[10] Ramulu P, Kennedy M, Xiong WH, Williams J, Cowan M, Blesh D, et al. Normal light response, photoreceptor integrity, and rhodopsin dephosphorylation in mice lacking both protein phosphatases with EF hands (PPEF-1 and PPEF-2). Mol Cell Biol 2001;21:8605–14.